Master's thesis

NTNU
Norwegian University of Science and Technology
Faculty of Medicine and Health Sciences
Kavli Institute for Systems Neuroscience

Janelle Shari Weir

Structural and functional dynamics of healthy and perturbed neuronal networks in vitro

Master's thesis in Neuroscience
Supervisor: Ioanna Sandvig, Ph. D; Axel Sandvig, MD, Ph. D;
Vibeke Devold Valderhaug (PhD candidate)
June 2019

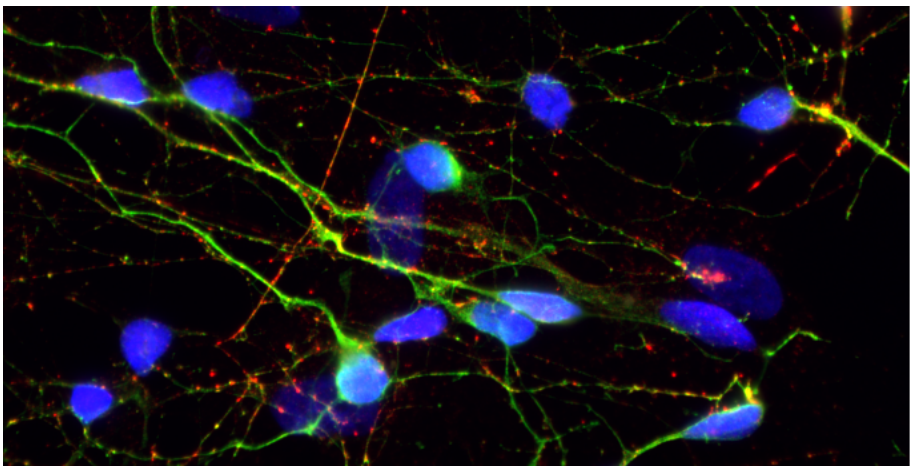

NTNU
Kunnskap for en bedre verden

Janelle Shari Weir

Structural and functional dynamics of healthy and perturbed neuronal networks in vitro

Master's thesis in Neuroscience
Supervisor: Ioanna Sandvig, Ph. D; Axel Sandvig, MD, Ph. D; Vibeke Devold Valderhaug (PhD candidate)
June 2019

Norwegian University of Science and Technology
Faculty of Medicine and Health Sciences
Kavli Institute for Systems Neuroscience

NTNU
Norwegian University of
Science and Technology

ABSTRACT

Rapid advancement in the field of morphogenic neuroengineering has led to interesting research perspectives in the area of *in vitro* neural network modeling using human induced pluripotent stem cell (hiPSC) derived neural lineage cells. When co-cultured with other cell types such as astrocytes, aspects of the *in vivo* environment are closely recapitulated so that hiPSCs can be maintained long term *in vitro* and retain their ability to differentiate and express neuron specific markers. Furthermore, hiPSC-derived neurons spontaneously form neural networks that have structural and functional relevance to *in vivo* systems. These networks exhibit dynamic spontaneous electrophysiological activity that can be monitored using state -of-the-art technologies such as microelectrode arrays (MEAs). This activity is highly stereotypical across multiple networks and is characterized by phase specific properties. In this study, we observed this stereotypical activity as an early primitive phase arising approximately between 07 and 14 days *in vitro* (DIV); a stable but complex phase of synchrony and network bursts; and finally, a decline phase. Furthermore, we perturbed the neural network via electrical stimulation that was applied through specific electrodes on the MEA. Results show that electrical stimulation completely disrupted endogenous global synchronicity immediately in the neural network as quickly as 20 minutes post perturbation. Furthermore, network synchronization with a distinct temporal structure similar to the applied stimulation persisted in the neural network up to 48 hours post repeated stimulation, thus suggesting an adaptive learning response, which may be indicative of an interplay between Hebbian plasticity, as well as homeostatic plasticity mechanisms. The overarching conclusion of this work is that *in vitro* models of neural systems on MEAs are relevant for the study of complex neural network behaviours and may be beneficial for studying the interrelated dynamics of Hebbian and homeostatic plasticity that work in tandem to sculpt network behaviour in response to perturbation.

ACKNOWLEDGEMENT

Special thanks to NTNU and the Translational and Regenerative Neuroscience Group.

I would like to express great appreciation to my research supervisors Ioanna Sandvig (Ph. D) and Axel Sandvig (Ph. D, MD), for giving me the opportunity to complete my master's thesis in their group. Thank you for tailoring a project that taught me so many invaluable and applicable research techniques, as well as afforded me the research independence I needed to think critically. Your immense knowledge during the planning, development and execution of this research work, coupled with your useful critiques and constructive recommendations, have been much appreciated.

I am particularly grateful to my co-supervisor, Vibeke Devold Valderhaug (PhD candidate) for her patient guidance and willingness to give her time so freely to answer every question I had. Thank you for the hours of lab training, your enthusiastic encouragement and insightful recommendations necessary to keep my progress on schedule.

My special thanks are extended to the other PhD candidates in the lab, Ola Huse Ramstad, Ulrich Stefan Bauer, Lars Schiro and Vegard Fiskum for their encouragement and overall helpfulness. Together, you have all lightened the journey to completing this thesis with great lunch conversations, groovy tunes and the worst yet most hilarious puns ever (looking at you Vegard).

I am extremely grateful to my mother and sisters for their continued support in all my life decisions, even though it usually means supporting me journeying off to another continent and not seeing them for years at a time. Thank you for reassuring me constantly that no matter where in the world I am and no matter how long it has been, I always have a place to return to. Your unshakable love has kept me mentally strong to keep pushing the borders of my comfort zone.

To my closest friend, Janvee - you'd be the best big sister if I ever had one. Thank you for your hard truths and loving support as my constant cheerleading team of 1. You are my lighthouse whenever I have doubts in myself. Thank you for your unconditional friendship, for your hours spent reading my drafts, for your constructive critiques and for the daily dose of memes.

Finally, to the great friends I found here in Norway, Madison and Gerard. You have always been there, keeping me sane when I need to get out and reconnect with the world. You guys are my disco balls.

TABLE OF CONTENTS

ABBREVIATIONS

ALS	Amyotrophic lateral sclerosis
AMPA	a- Amino-3-hydroxy-5-methyl-4-isoxazolepropionic acid
BBB	Blood-brain-barrier
BRN4	pOU domain, class 3, transcription factor 4
CaMKII	Calcium (Ca2+)/ calmodulin-dependent protein kinase II
CLIP2	CAP-Gly domain containing linker protein 2
c-MYC	MYC proto-oncogene, BHLH transcription factor
CNS	Central nervous system
DAPI	4',6-diamidino-2-phyenylindole
DIV	Days *in vitro*
D-MEM	Dulbecco's modified eagle medium
DNA	Deoxyribonucleic acid
D-PBS	Dulbecco's phosphate-buffered saline
E47	Transcription factor 3
EGF	Epidermal growth factor
EthD-1	Ethidium homodimer-1
FBS	Fetal bovine serum
FEZf2	FEZ family zinc finger 2
FGF2	Fibroblast growth factor 2
GABA	Gamma-aminobutyric acid
GDNF	Glial cell derived neurotrophic factor
GFAP	Glial fibrillary acidic protein
HDF5	Hierarchical Data Format
hiPSC	Human induced pluripotent stem cell
iPSC	Induced pluripotent stem cell
ISI	Interspike interval
KLF4	Kruppel like factor 4
LIN28	Lin-28 homolog A
LTD	Long-term depression
LTP	Long-term potentiation
MATLAB	Matrix Laboratory
MBR	Mean burst rate
MEA	Microelectrode array
MFR	Mean firing rate
NANOG	Nanog homeobox

NEUN	Neuronal nuclei
NEX	Nexon system file format
NLS	Neural lineage stem (cells)
NMDA	N-methyl-D-aspartate
NSC	Neural stem cell
OCT4	Organic cation/carnitine transporter 4
PSD-95	Post-synaptic density 95
SATB2	SATB homeobox 2
SMA	Spinal muscular atrophy
SOX2/5	SRY (sex determining region Y)-box 2/5
SVZ	Sub-ventricular zone
TGF-a	Transforming growth factor alpha
TSP	Thrombospondin
TUJ	Beta III tubulin
VZ	Ventricular zone

1. OVERVIEW

1.1 Neural network and plasticity

Communication within brain regions and between neural systems requires an intrinsic network structure that is self-organizing and self-regulating, and which also undergoes neuromodulation that affects the network in different ways. Neural plasticity is concerned with the nervous system and its capacity to functionally and structurally modify itself in response to endogenous or exogeneous experience [1]. It is a crucial component of neural development and ensures normal network functioning and adaptability to variable intrinsic or extrinsic stimuli, aging, or pathology. The investigation of plasticity is extensive but has converged to classify at least two major processes taking place. On the one hand, there is activity-dependent functional plasticity (Hebbian plasticity) that works to regulate the transmission efficacy of existing synapses, and on the other, there is structural plasticity (homeostatic plasticity) which entails morphological changes in connectivity [2]. Together, they coordinate to assure network integrity.

These processes make up the underlying factors in learning and memory, with early intuitions proposing plasticity to be the driving force behind the morphological synaptic changes which enable learning. Hebbian theory states that neurons that are persistently excited together or are responsible for the firing of another neuron, increase the efficacy of these interrelated neurons being ‘wired’ in the network together [3]. This implies that the structure of the neural network is not fixed throughout adulthood but rather dynamic and malleable beyond the period of central nervous system (CNS) development. Research supporting Hebbian plasticity has found that functional networks are shaped by experience and depend on the level of neuronal activation [2]. In general, high level of neuronal activity result in stronger connections or long-term potentiation (LTP), and low level of neuronal activity result in weaker connections or long-term depression (LTD) [2,4,5]. This has led to numerous studies highlighting the molecular role of synaptic plasticity as an underlying component in learning and memory [6-11].

The concept of experience-dependent plasticity, where activity from one synapse drives the activity of another synapse and so on, implies that without regulation, the positive feedback loop can render the network unstable. This can occur when persistently high or low activity leads to persistent potentiation or depression respectively [2,12]. Therefore, compensatory mechanisms in the form of homeostatic plasticity were proposed as an intrinsic network counterbalance to Hebbian plasticity. These include mechanisms such as modification of ion channels density, regulation of neurotransmitter release, or removal and addition of synapses in response to activity dependent changes [12,13]. In addition, in response to network perturbation, synaptic scaling prevents firing rates from saturating during development and stabilizes synaptic strengths [14] in order to preserve functionality. Therefore, Hebbian plasticity is necessary for the neural network to acquire new functional properties, while homeostatic plasticity

preserves network homeostasis and stability, and maintains robust system functions in response to perturbation and uncertainty [15,16].

Despite the vast research into plasticity, the complexity of the mechanisms that govern neural network synaptic plasticity *in vivo* still remains largely unexplained. While the current research has advanced our understanding of the relationship between Hebbian and homeostatic plasticity mechanisms, there is still a need for more dynamic experimental and theoretical investigations into how each may foster or obstruct functional network restoration after perturbation. Using techniques that support a systems-level reductionist *in vitro* paradigm, we can directly observe evolving neural network dynamics, record network activity, and selectively modulate network plasticity to gain insight into their interactions.

2. INTRODUCTION

2.1 Development of cortical networks

2.1.1 Corticogenesis and neural development *in vivo*

Corticogenesis is a complex process of progenitor cell migration and differentiation aided by intrinsic and extrinsic environmentally inducive factors that direct the production of neurons in the different levels of the cortex [17-21]. Rapidly dividing progenitor radial glial cells in the ventricular zone (VZ) and subventricular zone (SVZ) in the developing cortex possess multipotent neural stem cell capabilities and are able to generate multiple cell types (Fig.1), including neurons that migrate to other parts of the nervous system [17,18,22]. The developmental fate of the neural progenitor is determined by a number of transcription factors (including Fezf2, Ctip2, Sox5 and Satb2) which may also influence corticocortical or callosal projection identity of pioneering neurons [17].

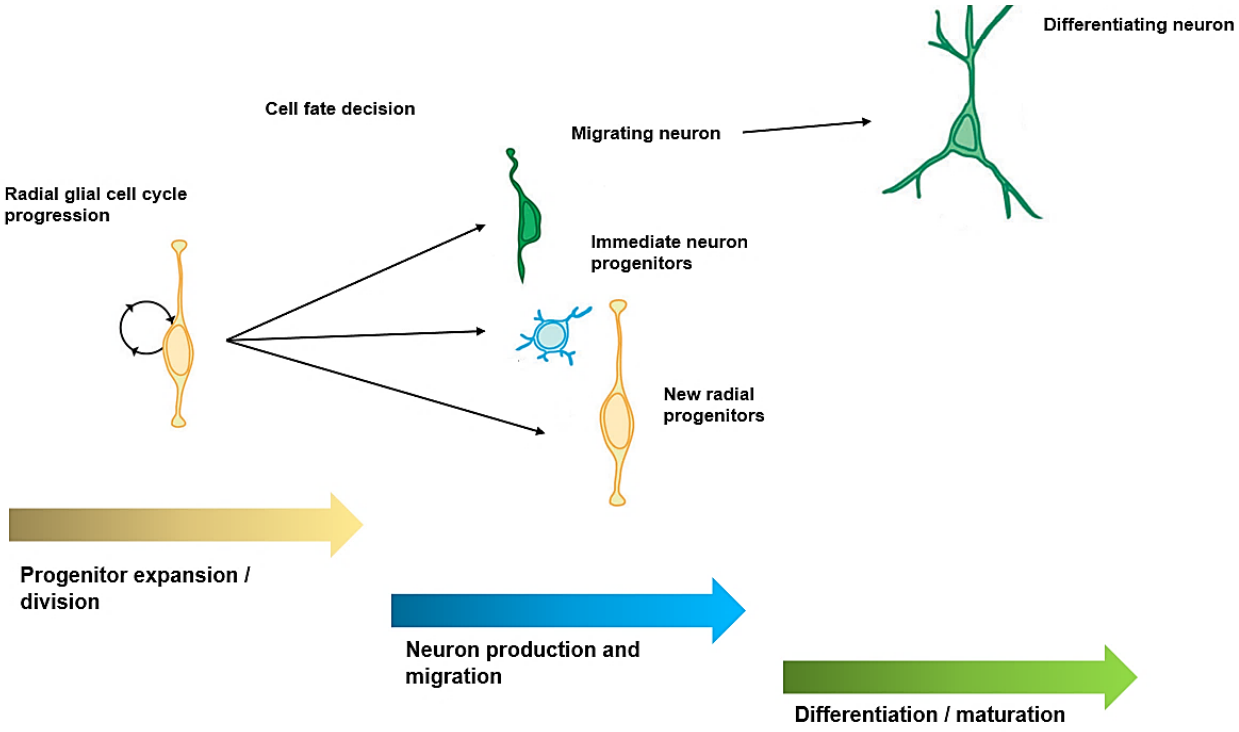

Figure 1. Schematic representation of cortical development. Adapted from Pilaz L & Silver DL. 2015 [22]. *Shown is the radial glial progenitor cell within the VZ that undergoes self-renewal division (curved arrow) to generate either neurons, intermediate progenitors that can also generate neurons, or new radial progenitors (straight arrows). As corticogenesis progresses, progenitors expand their populations and neurons migrate to form the different layers of the cortex in which they adapt a terminally differentiated fate.*

Corticogenesis is a time-limited process with the development of the CNS occurring rapidly from the first few postconceptional weeks to the third postnatal year, after which, expansion slows down dramatically and is followed by a rigorous process of refining maturing neural networks [23]. This involves synaptic maturation, synaptic pruning and apoptosis, gliogenesis and myelination, dendritic arborization and retraction, synaptic connectivity, neuroplasticity, and stabilized synaptic connections *in vivo* [23]. Several reports in the literature indicated that many of these developmental processes can be recapitulated *in vitro* [24]. By the end of corticogenesis, most cells in the nervous system will have completed stem cell division and are committed to a developmental fate. Therefore, adult neurogenesis is complicated by mechanistic concerns about the complexity of neurons, given their highly branching processes and polysynaptic connections, which make them terminally differentiated and unable to proliferate [25]. There are also further conceptual concerns about the ability of newly formed neurons to integrate into already existing circuits [25]. However, Hebbian plasticity theory strongly supports that adaptability in the neural circuit can be accomplished without requiring structural reorganization [3]. Moreover, reports have shown that in adulthood, the SVZ of the lateral ventricle and the subgranular zone in the dentate gyrus of the hippocampus have an evolutionarily conserved ability to generate new stem cells that may possess neuronal differentiation properties [26]. These neurogenetic niches continuously produce neuroblasts or progenitors of oligodendrocytes that migrate to other areas of the nervous system where they commit to their differentiated fate [27]. Notably, while only limited experiments have addressed whether these progenitors can be functionally integrated into the brain, the existence of these niches implies that the brain is not a static organ but instead one that relies on a complex coordination of endogenous plasticity mechanisms and structural flexibility in synaptic organization to maintain its function [27].

2.1.2 Modeling *in vitro* neural systems using neural lineage stem (NLS) cells

Recent developments in the field of morphogenetic neuroengineering have demonstrated that somatic cells can be converted to induced pluripotent stem cells (iPSC) with the induction of core transcription factors, namely KLF4, c-Myc, OCT4, SOX2 [28-31], NANOG, and LIN28 [32]. Later, it was found that human adult fibroblasts could be reprogrammed into iPSC (hiPSCs) that were similar to embryonic stem cells (ESC) in morphology, proliferation, surface antigens, gene expression, and epigenetic status of pluripotent cell-specific genes [29,30-32]. In the years following this discovery, hiPSCs have been reprogrammed from a wide range of cell types, using manifold combinations of inducive factors, resulting in the field burgeoning with exciting new perspectives for drug discovery, tissue and organ development, regenerative medicine, and systems modeling [33].

Thus, the field of human medical research is seeing a dramatic shift from the use of ESCs to iPSCs to circumvent the ethical concerns associated with the former [28]. Since iPSCs can be reprogrammed into various tissue and cell types from patient samples [34], they have potential for cell replacement therapies

in the treatment of diseases such as Parkinson's disease [35], amyotrophic lateral sclerosis (ALS) and spinal muscular atrophy (SMA) [36], without the significant concerns for immunological rejection as in ESC transplantation. Furthermore, research has confirmed that hiPSCs can be used *in vitro* to generate human neural stem/progenitor cells (NS/PCs), which can further be directly differentiated into specific neuron subtypes, such as dopaminergic neurons, motor neurons, cholinergic neurons, cortical neurons, and glial cells [30,31,37,38]. Another important discovery was that by using a combination of neural-lineage specific transcription factors, fibroblasts could be directly converted into neuron subtypes, effectively circumventing the pluripotent stage [39] (Fig. 2). One study used a 5-factor combination of compounds (Brn4, Sox2, Klf4, c-Myc, E47) to produce stable cell lines that expressed NSC markers, which had the ability to differentiate into either GABAergic, glutamatergic or cholinergic neurons and astrocytes, as well as express sodium channels to facilitate the generation of action potentials [40]. Thus, hiPSCs-derived neurons can be powerful alternatives, or complementary to animal models for studying human neural networks. Although animal models have greatly extended our understanding of the various molecular mechanisms of neurogenesis, maturity, and degeneration, they unfortunately do fall short in representing the human condition due to ontogenetic differences. As such, *in vitro* models of hiPSC NLS can be used in various applications, for example neurodegenerative diseases, to provide directly translatable clarification of naturally occurring human conditions.

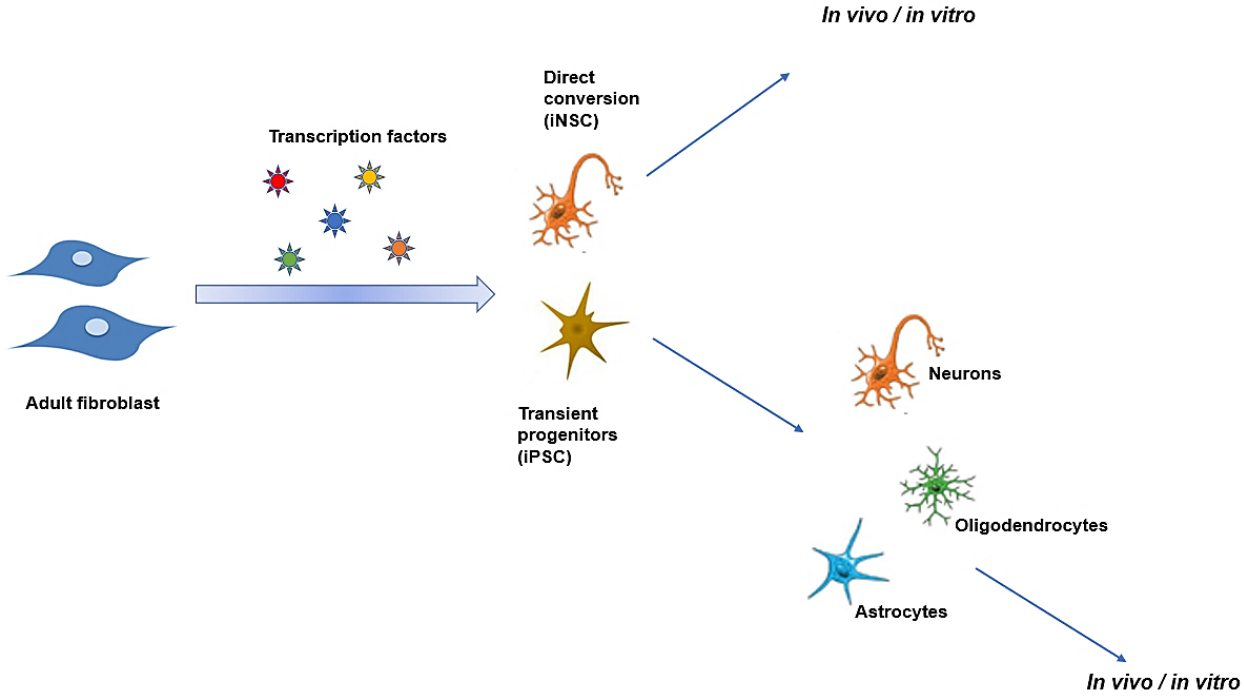

Figure 2. Schematic representation of reprogramming adult fibroblast. *By addition of defined transcription factors, adult fibroblasts can either be directly converted into induced neuronal stem cells (iNSC) or into induced pluripotent stem cells (iPSC). iPSCs have ESC-like properties and thus can differentiate into various neural cell types including neurons and glia.*

2.2 Modelling human neural networks *in vitro*

2.2.1 Establishing the *in vitro* neural network

Central to the entire discipline of neuroscience are the strict spatiotemporal sequence of corticogenesis and the functional optimization of neural networks, clearly, within the broader scope of CNS development and function. The structural organization of neural networks and the functional connectivity of synapses have been the basis for network neuroscience research for decades, with progressively more sophisticated empirical tools being developed to map, record, analyze, and model elements and interactions of neurobiological systems. When considering the enormous complexity of the adult brain, with several thousand cell types, billions of neurons and trillions of synaptic connections, it is almost impossible to explore neural networks on this large scale. Therefore, with advanced protocols, some of these complex structural and functional self-emergent properties of *in vivo* systems, including characteristic electrophysiological behaviours of neural networks can be selectively manipulated and monitored *in vitro* using neurons generated from iPSCs.

Neurons in a network relay information between themselves through intercellular transmission facilitated by synapses. The synapse is a junction between the pre and postsynaptic neuron over which signals propagate. Each neuron has a membrane potential, which is a difference in the electrochemical charge between the inside and the outside of the cell. Several ions play an important role in the membrane potential of neurons including positively charged sodium ions and negatively charged chloride ions that are predominantly extracellular (outside the cell); and positively charged potassium ions and negatively charged organic ions predominantly intracellular (inside the cell). At rest, the membrane potential is negative. Detection of a stimulus causes a transitory change in this ion gradient such that ions move across the membrane and cause membrane potential to become more positive and depolarize. When the depolarization reaches a threshold larger than the normal resting potential, an action potential occurs, followed by a repolarization back to baseline.

This electrophysiological activity of neurons can be measured both intracellularly (inside the cell membrane) and extracellularly (outside the cell membrane) [41]. Specifically, extracellular electrophysiological recording can be achieved using micro transducers which detect ion concentrations in their vicinity during an action potential. Furthermore, the electric field that is generated by ionic movement can be recorded by metal microelectrodes which measure the extracellular voltage produced due to an action potential [41]. Therefore, advanced technologies such as microelectrode arrays (MEA) have been established as a platform that can be used *in vitro* to study micro systems of electrophysiological cells. Cells are grown on top of a glass substrate on the MEA that is embedded with electrically independent metal electrodes so that any action potential within measurable vicinity of an electrode is captured [41,42]. MEAs conveniently provide the opportunity to assess dynamic *in vitro*

neural network activity patterns such as the rate of action potentials (spikes) and groups of spikes (bursts) recorded on each electrode, as well as, export this data to software such as Neuroexplorer in order to analyze network features, for example burst duration, number and percentage of spikes in a burst, interspike and interburst intervals [43]. Additionally, some MEAs have bidirectional functionalities enabling simultaneous high spatio-temporal multisite recordings of network electrical signals, as well as the ability to selectively stimulate sites in the cultured network to elicit a response [41-43]. Importantly, with appropriate care, *in vitro* neural networks can be maintained on MEAs in an incubator for several months thus allowing the researcher to gather data at different points during maturity in order to denote a developmental profile.

Maintaining an optimal microenvironment for developing neural networks *in vitro* is paramount because the brain relies on an intricately designed neural architecture in order to provide the scaffolding needed to support its dynamic functional and structural synaptic functions [44]. Accordingly, in order to sustain iPSC-derived neural lineage cells during their differentiation into mature neurons, other neural cell types such as astrocytes may contribute to the physiological relevance of the *in vitro* microenvironment [38]. There is a large volume of published literature describing how co-culturing with astrocytes can promote neuronal attachment, growth, and survival [45,46] directly relating to the *in vivo* role of astrocytes in regulating ion homeostasis, providing metabolic support for developing neurons, secreting bioactive molecules including transforming growth factor alpha (TGF-*α*) and glial-derived neurotrophic factor (GDNF) to control the blood-brain-barrier (BBB), and neurotropic factors including neuropeptides [47]. Astrocytes are also involved in synaptic modification through the control of development and maintenance of synaptic areas, and thus affecting synaptic strength and plasticity [48]. Astrocytic substances *in vitro* such as thrombospondins (TSP) (among others) may also influence synaptic formation, refinement, and maturation [49-51].

2.2.2 Intrinsic development properties of modeled neural networks on MEAs

First and foremost, developing neural circuits are self-organizing and exhibit emergent behaviour. In other words, developing neurons derive synapses and develop spontaneous electrical behaviour in the absence of external manipulations or sensory input [52]. *In vivo*, the immature neural network is characterized by primitive overconnectivity and emergent network-driven activity, which serve to establish the synapses and structural connections necessary for function and survival [52,53]. This arrangement directs the configuration of the developing network in an experience-dependent manner, enabling it to accommodate dynamically to changing inputs during maturation [44,53]. As mentioned earlier in section 2.1.2, many of the current studies emphasize that iPSC-derived neurons *in vitro* maintain intrinsic morphological properties as those found in ESCs. Therefore, hiPSC-derived neurons can develop to achieve self-organized connected neural networks that exhibit spontaneous electrophysiological activity

similar to those found in *in vivo* [33,54,55]. These endogenous electrophysiological characteristics of maturing neural networks on MEAs can be converted into easily observable digital signals so that information about the basic spatial and temporal aspects of the network´s functional activity can be obtained [43].

Comparable to *in vivo* neural networks, the electrophysiological activity of *in vitro* neural networks detected using MEA reveal a highly stereotypical repertoire of behaviour over the course of network development. There is also an unambiguous relationship between the emergence and evolution of spontaneous synaptic activity and age of the neural network. The majority of studies have found that simple electrophysiological activity arises as early as 5-7 days *in vitro* (DIV) and becomes more complex with periods of overall activity increase, peak periods, plateaus of minimal increase or decrease in activity, and significant declines in action potentials as the network matures [24,46,56-59]. These findings appear to recapitulate some aspects of key activity patterns observed *in vivo* [60-66]. Additionally, stereotypical features of developing human neural networks such as network bursts [67] are identified as an indication of synaptic development, signaling and network functionality, as well as information processing and neuroplasticity [68].

2.3 Neural network plasticity *in vitro*

2.3.1 Hebbian plasticity

Regarding plasticity mechanisms, even though neural circuits appear well established beyond the period of cortical development *in vivo*, experience-dependent plasticity still plays a vital role in incorporating new behavioral patterns into the network. The pioneering intuitions of Hebb in 1949 have led to the understanding that synaptic plasticity reshapes the strength of information flow between presynaptic and postsynaptic neurons [3]. The result of this is a modification in the likelihood that presynaptic activity will result in postsynaptic activity [4], thus facilitating local circuit refinement to support memory and learning in neural networks, and as such, in the CNS.

One major experimental issue with studying cortical assemblies *in vitro* is the highly variable ongoing synaptic activity that is almost always irregular across similarly prepared neural networks and even across recordings of the same neural network which makes comparability between cultures difficult. Additionally, because neural networks develop spontaneous activity in the absence of sensory input, this makes it difficult to identify “behavioural output” that is relatable to *in vivo* neural systems. This poses limitations in direct generalizability since developing *in vivo* neural systems receive sensory inputs that can be successfully incorporated into existing brain circuitry that drives behavioural output and can be interpreted in the context of neural network plasticity.

These factors have led to the development of several plasticity protocols using appropriate high frequency sequence of individual tetanic electrical stimulations (50 - 200Hz) on MEAs to modulate the activity of *in vitro* assemblies [69-72] and produce a “behavioural output”. The seminal publication by Bliss and Lomo in 1973 provided evidence of neural plasticity changes as a result of direct electrical stimulations to a subset of neurons in the perforant pathway in a rabbit. Their publication described a rapid build-up of spikes immediately after the stimulation, which was followed by a period of reduced spiking and then a subsequent potentiation (LTP) lasting up to several hours [4]. Similarly, long-term depression (LTD), in a similar manner to LTP, was found to be induced in the hippocampus by long periods of stimulation at lower frequencies than those used to induce LTP and resulted in decreased synaptic strength below initial network baseline [73,74]. Similar investigations with network-wide electrical stimulation patterns reported that post stimulation, the neural network could exhibit either a potentiated response with increase spiking [69,70], synaptic depression [70], or functional connectivity changes [72].

Numerous studies have also specified that the susceptibility of the synaptic changes favoring LTP or LTD is determined by the relative timing between pre and postsynaptic activity [12,75,76]. Early studies found that repetitive postsynaptic spiking within a 20 ms time window after presynaptic activation resulted in LTP, whereas postsynaptic spiking within a window of 20 ms before the repetitive presynaptic activation led to LTD [77]. Furthermore, LTP has been classified in time-specific phases where early LTP is claimed to occur within the first 30 minutes of persistent activity and lasts for a relatively short time from 30 minutes to 2 hours, while late LTP lasts many hours to days post-robust synaptic activation [2,5,78-80]. This indicates that electrical stimulation can provide the “sensory stimulus” that *in vitro* neural networks inherently lack, to induce neuroplasticity changes that can possibly clarify how information is integrated in the circuit.

These publications on applied electrical stimulations provided valuable insights for neuroscientists about the mechanisms for learning and information storage in the brain. They also contributed to the vast and still growing research on the cellular and molecular aspects of synaptic plasticity [10,13,77,81,82], especially those governing functional Hebbian modifications. However, since strengthening mechanisms are dependent on coincidental firing between the pre and postsynaptic neurons, over time, a positive feedback loop can emerge (Fig. 3). As mentioned earlier, this can either further increase the potentiated activity within the network and very rapidly result in loss of circuit functionality [83,84] either by synaptic saturation or neural population silencing [85-87], or could lead to effects such as loss of dendritic spines or separation of synapses in response to very low firing rates [88]. From a functional perspective, it seems necessary to have an intrinsic counteracting homeostasis system to deal with Hebbian stability concerns. This means, both forms of plasticity need to be considered, especially in the *in vitro* context if the neural circuit is manipulated to produce changes in behaviour.

2.3.2. Homeostatic plasticity

Considering the above, homeostatic plasticity has been termed as a negative feedback process where synaptic efficacies are decreased in persistently high activity and increased in persistently low activity [2]. This occurs through synaptic scaling to compensate for activity that could otherwise result in neuronal/network dysfunction [2,12,83,89,90] (Fig. 3). Studies have revealed a complex coordination of signaling processes maintaining network activity within a dynamic range. Although geared towards different goals, both types of plasticity share overlapping components in molecular pathways, such as receptor trafficking, so that homeostatic responses in a neural circuit may be expressed as lasting structural and synaptic changes that impact the circuit's capacity for subsequent Hebbian plasticity [91].

Various homeostatic mechanisms have been identified which appropriately coordinate total network excitation and inhibition, and maintain population synapses within optimal bounds [12,84,85,92-100]. However, synaptic scaling is the most studied form of homeostatic plasticity and involves structural adjustment of the entire network in an orchestrated fashion such that activity is either scaled up or scaled down [14,100-102] in response to chronically low or elevated network activity respectively. This process includes modification at glutamatergic synapses, such as changes in NMDA presence, AMPA trafficking, kinase/ phosphatase activation, formation or removal of synapses [2,14]. Downregulating synaptic scaling helps the conductance to not exceed the capacity of the neuron, thereby keeping it within a healthy and stable range. Moreover, synaptic scaling also plays a crucial role in preventing unnecessary synaptic loss by increasing synaptic strength during chronic activity suppression [84].

Finally, since homeostatic plasticity exists to maintain activity equilibrium in the neural network, it may play a vital role in preserving network stability in the event of electrical stimulation-induced perturbation. As was pointed out in the previous section, electrical stimulation of the *in vitro* neural network changes the electrophysiological behaviour of the neural network from its normal state (i.e. induces a perturbation) and results in a reorganization of firing behaviour. The studies also show that in many cases, the neural network maintains functionality even after reorganization. This provides strong evidence that *in vitro* neural assemblies, like *in vivo* assemblies may be inherently adaptable to perturbation, although more research is needed to clarify this.

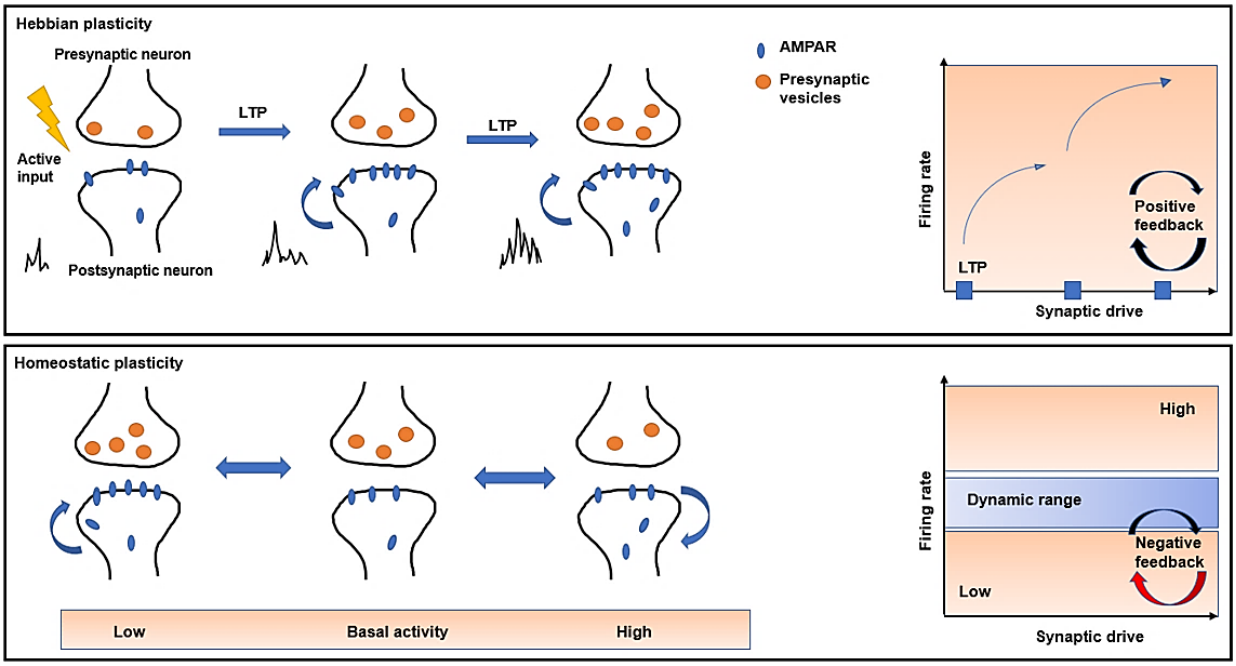

Figure 3. Schematic representation of the interplay between Hebbian and homeostatic mechanisms at an excitatory synapse. Adapted from Fernandes D & Carvalho AL.2016 [84]. *Hebbian plasticity mechanism such as LTP induce long lasting changes in the synaptic strength which can destabilize the neural circuit in a positive feedback loop. Conversely, homeostatic plasticity operates in a negative feedback way to compensate for prolonged activity changes and thus stabilize neuron / network activity within a dynamic physiological range*.

2.4. Final note

Taken together, models of *in vitro* neural circuits allow the researcher to reduce the complexity of neural network mechanisms in the brain, thereby facilitating research into specific components of neuroplasticity. By interfacing hiPSC derived neurons with MEAs, we can monitor the morphological and functional development of the network long term. In addition, the MEA technology makes it possible to characterize some aspects of electrophysiological dynamics of neural networks such as spike profile and bursting behaviour. Finally, by applying electrical stimulation through the MEAs, the neural network responses to the stimulus can be shaped and studied to provide insight into network adaptability, learning and information transmission. This can further highlight *in vitro* features of Hebbian and homeostatic plasticity mechanisms that are characteristic in the *in vivo* context and therefore can make *in vitro* neural networks more comparable to *in vivo* neural networks. This approach may also help find answers to key questions concerning neural network structural and functional response to perturbations.

3. AIMS AND OBJECTIVES

The aim of this MSc project was to recapitulate morphological and electrophysiological properties of neural network development *in vitro* using hiPSC-derived neurons and to investigate neuroplastic responses to electrical stimulation-induced perturbations in the *in vitro* neural network.

The main objectives were:

I. Establish hiPSC-derived neural networks on standard microelectrode arrays (MEAs)
II. Maintain *in vitro* networks so they can achieve morphological maturity
III. Monitor the development of spontaneous electrophysiological neural network activity long term (>21 DIV)
IV. Perturb the neural network by applying electrical stimulation and assess the neuroplastic response

Research Questions:

1. Does the hiPSC *in vitro* neural network recapitulate stereotypical aspects of neural network development found *in vivo*, such as neurogenesis and synaptogenesis?
2. Are there emergent, electrophysiological activity traits that signify distinctions between developmental stages?
3. Does the neural network exhibit a response to electrical stimulation?
4. Can the neural network adapt to perturbations in a manner that suggests functionality?
5. Can the experimental setup allow for observation of plasticity related responses such as LTP and LTD?

Hypotheses:

1. hiPSC-derived neurons self-organize and exhibit age-dependent electrophysiological properties comparable to those found *in vivo*
2. Direct electrical stimulation will elicit an increase in the electrophysiological activity from baseline recording
3. There will be an increase in global network activity post stimulation that is greater than the spontaneous activity pre stimulation
4. The neural network will restore electrophysiological activity to a stable state post stimulation
5. Indication of Hebbian modification will be reflected in the network as changes in the timescale of firing to mimic that of the stimulation temporal sequence

4. MATERIALS AND METHODS

4.1 Methods for monitoring the electrophysiological activity of in vitro neural networks

In vitro neural networks were established and studied using commercially available microelectrode arrays (MEAs). The standard microelectrode array (MEA60 200/30 iR TiN) (Multichannel System ™) contains 60 electrodes embedded in a glass substrate in a glass ring chamber that has an internal diameter of 19mm, an external diameter of 24mm, and a height of 6mm. The 60 Titanium nitrate electrodes are organized in an 8x8 pattern. There are 59 recording electrodes of 30µm diameter, separated by 200µm. One electrode serves as an internal reference and is located in the middle of the leftmost column. The internal reference electrode does not record or stimulate. Neural networks are grown on top of the electrodes on a silicon nitrate isolation layer with a glass substrate. This enables recording of the electrophysiological activity of the cells directly on top of or within the vicinity (50-100µm area) of each electrode.

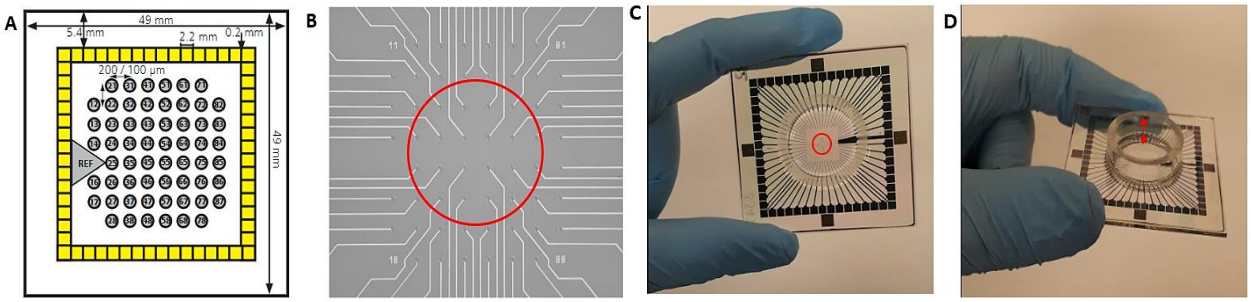

Figure 4. The standard MEA60 200/30 iR TiN. *(A) The number of each electrode (grey circles) follows the standard numbering scheme for square grids such that the first digit represents the column number while the second digit represents the row number. The yellow grid bordering the electrodes has specified MEA pin numbers which are channel numbers used in the data acquisition program. The desired cell seeding area on the surface of the MEA is demarcated with a red circle (B-C). D) The ring chamber is 6mm in height with a volumetric capacity of approximately 500µl. Images A-B reprinted from Multi Channels MEA2100 SystemTM Manual 2016.*

The MEAs can be used to selectively stimulate the *in vitro* neural network electrically through individual electrodes, or by selecting specific groups of electrodes. In addition, MEAs are compatible with chemical and optogenetic stimulation.

The MEA2100 System ™ allows for extracellular recordings from the MEA and consists of two main devices. One is the interface board with an integrated signal processor and the other is the MEA IT60 headstage equipped with integrated amplification, signal processor, analog-to-digital (A/D) converter and stimulus generator. The system also consists of a temperature control sitting underneath the MEA recording stage that maintains the culture temperature constantly at 37^{o}C whilst recording (Multi Channel Systems; Reutlingen ™). In addition, the Multi-Channel Suite contains the software for electrophysiological data acquisition and analysis. It is made up of four independent programs; Multi-Channel Experimenter for online recording, Multi-Channel Analyzer for offline data analysis of experimenter files, Multichannel

Video Control, and Multi-Channel DataManager for data export supported by Matlab, Python or Neuroexplorer.

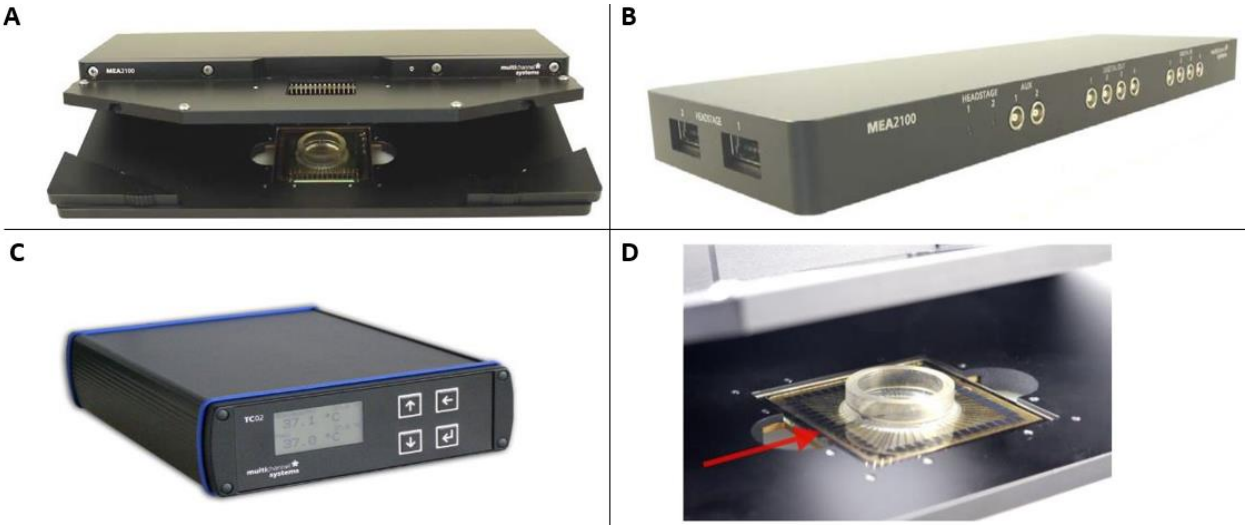

***Figure 5.* MEA2100-System.** *A) MEA IT60 Headstage which contains the contact unit for the MEA. B) MEA Interface board containing integrated signal processor. C) MEA2100 Temperature controller TC 01/02 with a PT100 sensor which when connected, guarantees constant temperature conditions for the culture sample placed in the headstage. D) Open lid of MEA2100 headstage with MEA inside. The MEA is not symmetrical so the correct orientation is with the reference electrode to the left side of the headstage as indicated by the red arrow. Images A-D reprinted from Multi Channels MEA2100 SystemTM Manual 2016.*

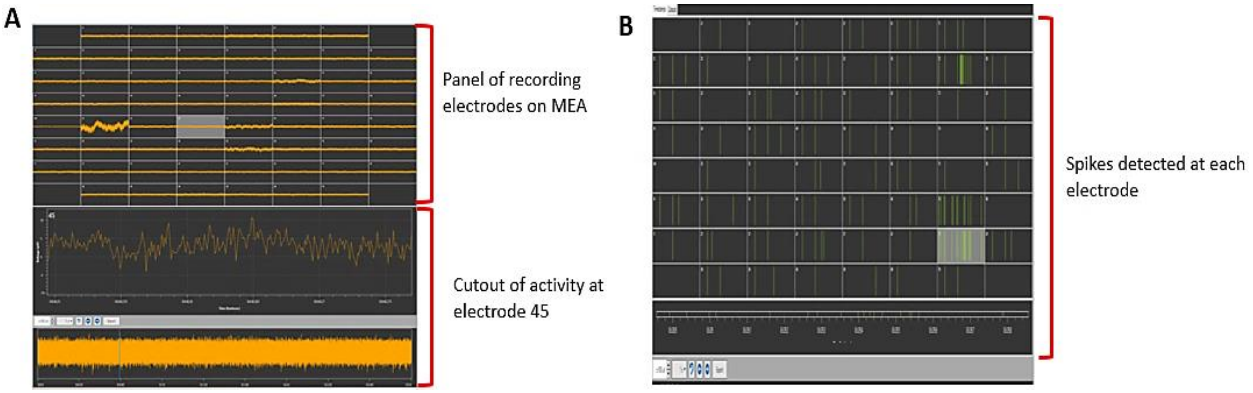

Figure 6. Example of data online experimenter program during recording (A) and the spike detector (B).

4. 2 MEA preparation

4.2.1 Impedance Testing

To ensure that the selected MEAs (standard *n=3)* were viable for recording and culturing, the surfaces were first examined under a microscope to make sure they were debris free and had no visibly damaged electrodes. Afterwards, the impedance was measured with the MEA IT program (*Multichannel Experimenter*) using Dulbecco's phosphate-buffered saline (D-PBS) as conductor and an external silver

electrode reference. The MEA culture chambers were filled with 1 mL of D-PBS. The external reference electrode was placed in the PBS solution so that the tip was submerged but not touching the MEA culture surface. On the computer, the MEA ID number was recorded and the correct layout selected (MEA60 200/30 iR TiN) before testing commenced. A normal impedance is below 250Ω, with the internal reference electrode below 5Ω. The impedance for all selected MEA was below 200Ω.

4.2.2 Pre-treatment

In the laminar flow hood, 1 mL of 70 % isopropanol was added to each MEA cell culture chamber for 10 seconds each. This was then removed, and each chamber was rinsed x5 with sterilized water. MEAs were left in a petri dish in the laminar flow hood overnight for UV treatment.

4.2.3 Hydrophilic treatment

Once MEAs were treated, the normal hydrophobic surface needed to become hydrophilic to ensure cell attachment. This was achieved by adding 1 mL of fetal bovine serum (FBS) (*Invitrogen ™, Thermo Fisher Scientific*) and incubating for 1hr at 37º in a 5% CO2/ 95% air atmosphere. After incubation, the FBS was removed and the chamber rinsed x3 with sterile water. Matrigel (*VWR, Corning*) was used to coat the surface of the MEAs at a concentration of 1:10 / Matrigel: Neural Expansion XF Media (*Axol Bioscience Inc.*)

4.2.4 Extracellular recording

A teflon membrane cap fitted onto the MEA prevented exposure of the culture to the air while recording. To compensate for any initial voltage drift in the system, a 1-minute lapse was allowed for the data acquisition before the start of recording. The Multi-Channel experimenter enables electrophysiological data to be acquired in real-time at a sampling rate of 10,000 kHz. The electrophysiological activity of the neurons in the network was filtered by a built-in system, Butterworth, with a high pass cutoff at 200Hz to obtained the local field potential (LFP) at each electrode. An amplitude threshold for spike detection was set at 5.0 standard deviations (std) above the threshold and -5.0 std below the threshold. The system records the field potential from the 59 recording electrodes simultaneously. Raw data visualization was also possible using the Spike Detector tabs in the experimenter program with each electrode having a unique rising and falling threshold that is dependent on the level of background noise. The data presented were obtained from 3 neural networks monitored once per week for 8 consecutive weeks under the same conditions. The recordings were made at random intervals and the data from all the electrodes for each period of development were used, including those electrodes that registered no activity at some periods, to generate the results.

4.3 Culture of astrocytes and hiPSC-derived neural stem cells

Approximately 5000 rat primary cortical astrocytes at passage number 7 (*Invitrogen ™, Thermo Fisher Scientific N7745-100*) were cultured onto each standard MEA60 in a DMEM high glucose media (*Glibco ™, Thermo Fisher Scientific, 11995-065*). The media were supplemented with 15% v/v FBS (16000-036) and 10µl/mL penicillin/streptomycin (*both from Invitrogen ™, Thermo Fisher Scientific*). After 2 days in vitro (DIV), the astrocyte media was removed and the chambers rinsed with D-PBS and replaced with neural expansion XF media (*ax0030-500, Axol Bioscience Inc.*) supplemented with 20ng/mL Recombinant Human FGF2 (ax0047) and 20ng/mL Recombinant Human EGF (ax0048), as well as 1µl/mL rock inhibitor (*Y-27632, Invitrogen*).

The hiPSC- derived neural stem cells (H9N) passage number 2 (hyCCNs; ax0019, *Axol Bioscience Inc., UK)* were retrieved from the -80°C freezer and thawed in a 37°C water bath for about 2 minutes. In the laminar flow hood, the H9N neural lineage cells were transferred dropwise from the cryovial to a centrifuge tube containing 8mL of prewarmed spinning media comprised of 10mL Knockout DMEM/F12 and 100ul knockout serum. Cells were centrifuged at 200 x g for 5 minutes. Afterward, the supernatant was removed completely, and cells resuspended in 1mL of prewarmed neural expansion XF media (*ax0030-500, Axol Bioscience Inc.*). The total number of cells was determined in suspension via hemocytometer count and about 70,000 cells were seeded onto the astrocyte feeder layer for each MEA60. After 4 days, the cell media were switched to Neural Differentiation XF Medium (ax0034-125). Henceforth, based on the manufacture's master protocol (*Axol Bioscience, neural stem cell master protocol version 5.0*), cells should synchronously differentiate into a pure population of cerebral cortical neurons. Neurons were maintained in Neural Maintenance XF Medium 9 days later. All media were supplemented with 100µl/mL penicillin-streptomycin prior to use. To prevent evaporation, MEAs were kept in petri dishes sealed with parafilm in a standard humidified air incubator (5% CO2, 20% O2, 37°C) at all times. Half of all media were exchanged every 3 to 4 days.

4.4 Live/Dead Assay

Concurrently with the cultures of human-induced PSC-derived neurons on the MEA, equivalent astrocyte-neuron co-cultures were kept on coverslips. The methods for maintenance and schedules for media change were identical. At 14 DIV, a live/dead viability/cytotoxicity assay (*L3224, Invitrogen ™*) was carried out to determine the viability of the neuronal culture before immunocytochemistry was performed. This assay simultaneously uses membrane permeable Calcein-AM and membrane impermeable ethidium homodimer-1 (EthD-1) to stain viable and dead cells respectively. The DNA of dying and dead cells are stained by the red fluorescent dye, while the live cells are labeled using a green fluorescent dye. The fluorescent calcein-AM enters cells and interacts with intracellular esterase activity causing it to be

visualized as fluorescent calcein. The staining solution was prepared by adding 0.8µl of Ethidium Homodimer-1-stock solution and 0.4µl Calcein-stock solution to 2 mL D-PBS. This was added to the counting wells and cells incubated for 40 mins covered with aluminum foil at room temperature in the laminar flow hood. Cultures were inspected under a fluorescent microscope.

4.5 Immunocytochemistry and imaging

After the live /dead assay, coverslip samples were fixed with 2% paraformaldehyde (P6148, *Sigma*) in maintenance media for 5 minutes at room temperature, followed by 4% paraformaldehyde only for 20 minutes. After a period of 3 washes with PBS for 10 minutes each, a blocking solution made up of 5% goat serum and 0.3% Triton X in PBS solution was added for 2 hours at room temperature. A staining solution of 1% goat serum and 0.1% Triton X in PBS was prepared and the primary antibodies added to this. The primaries used were chicken anti-GFAP at dilution 1:1000 (ab4674, *Abcam),* to label astrocytes, rabbit anti-synaptophysin at dilution 1:250 (ab32127, *Abcam*) for specific labeling of synaptic vesicles as a presynaptic marker, mouse anti-β-tubulin (TUJ) at dilution 1:1000 (ab41489, *Abcam*) for specific labeling of neurons, mouse anti-PSD95 at dilution 1:300 (ab13552, *Abcam*) to label postsynaptic junctions, mouse anti NeuN- neuronal marker at dilution 1:1000 (ab104224, *Abcam)* and rabbit anti nicotinic acetylcholine R a1 at dilution 1:50 (ab221868, *Abcam*).

After removing the blocking solution from the wells, 500µl of the primary solution was added to each well, and the cells were left for 24hrs at 8^{o}C wrapped in parafilm on a rotating plate. Afterward, fixed cells were washed 3 times with D-PBS for 10 minutes each at room temperature. To visualize the immunolabeling, 500µl secondary antibodies were added to the washed cells. The secondaries used were goat-anti-chicken 647 Alexa Fluor (A-21449, *Life Technologies*), goat-anti-mouse 488 Alexa Fluor (A-11001, *Life Technologies*), and anti-rabbit 568 Alexa Fluor (A-11079, *Life Technologies*) for 2 hrs at room temperature in the dark, all at dilution 1:1000. In addition, the secondaries were removed from one of the wells and the fixed cells washed 1x with D-PBS. To stain the axons and dendrites of the fixed neurons, phalloidin at dilution 1:500 in D-PBS was added to this well for 20 minutes and washed once before all cell nuclei were counterstained by adding 500µl Hoesch dilution 1:10000 in PBS. Cells were washed 3 times with D-PBS and the coverslips were mounted on glass microscope slides using Fluoroshield.

Phase contrast images of neural networks were obtained using a microscope (*Zeiss Axio Vert. 25)*. Imaging for immunoassay was done using a fluorescent contrast microscope (*Zeiss Axio Vert. A1)*. All images were processed using Image J software (NIH), Microsoft Paint and Microsoft Powerpoint.

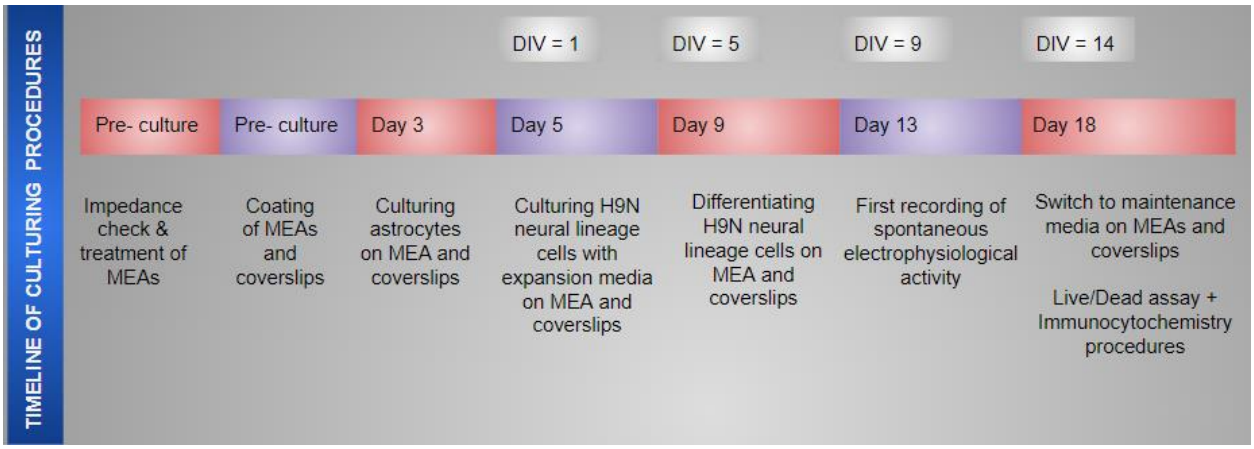

***Figure 7*. Simple timeline of culture procedures.** The above timeline illustrates the process from MEA impedance testing, to culturing, differentiating, and maintaining the neural network. It also shows when the live/dead cytotoxicity assay was done. Furthermore, the first of 8 recordings of spontaneous electrophysiological activity are shown here. Note that 'Day' refers to the day from the start of the experiment including the process of treating the MEAs, while 'DIV' refers to the day since seeding/ culturing the neural network.

4.6 Protocol for electrical stimulation

Electrical stimulation of the *in vitro* neural network was carried out for three consecutive days from 57 DIV. Only one network was selected for electrical stimulation (Network 3), and the other two *in vitro* neural networks were maintained with no applied stimulation. Two stimulating points were selected from Network 3, at electrodes that exhibited the highest mean firing rates (MFR) identified from the most recent recording of spontaneous activity. A monophasic stimulation of 10Hz at -200mV was applied twice each day for 15 minutes, with 10 minutes between each new session of stimulation. Stimulation recordings were made from the electrodes surrounding the stimulated electrode, and not the stimulating electrode itself. Like the recordings done for spontaneous activity, a one-minute lapse was allowed before commencing the recording to capture only the marked changes due to stimulation. Recordings of 10 minutes of network activity were taken 20 minutes post stimulation. These 20-minutes-post recordings were only taken after the second session of stimulations. Similarly, 5-minute recordings were taken 24 hours post stimulations (on successive days of the experiment). The analysis of the data was carried out using Neuroexplorer *(NEX Technologies)* and MATLAB *(Mathworks Inc.)*.

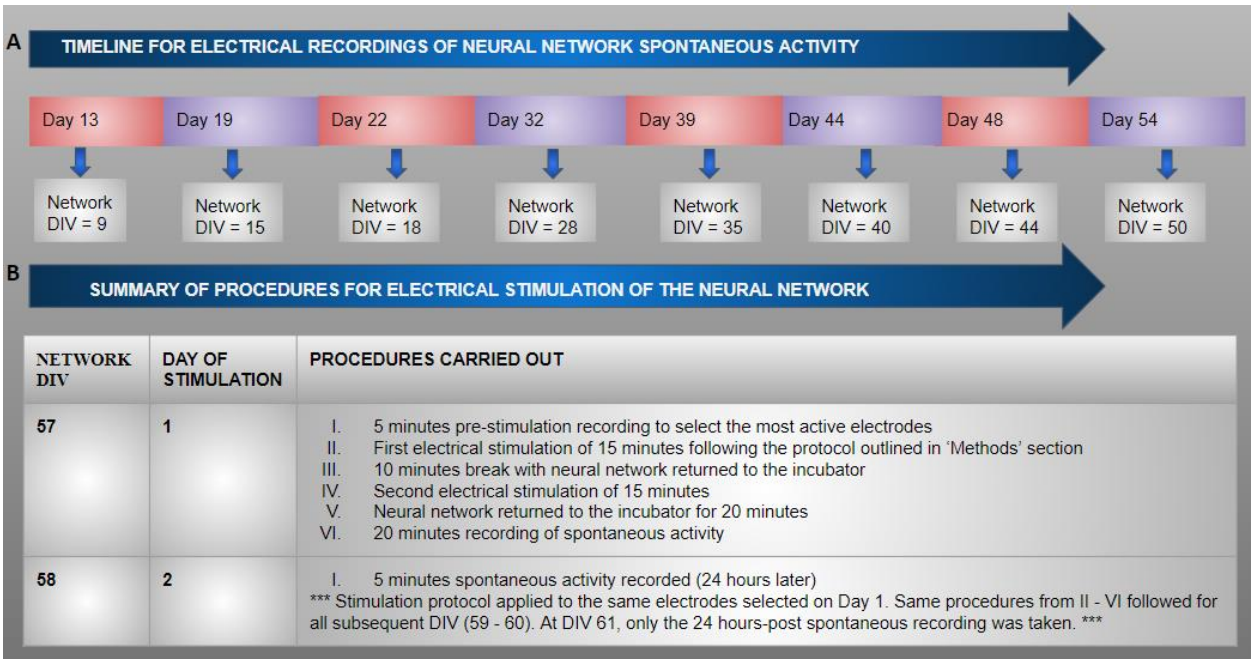

Figure 8. Simple timeline of recordings of spontaneous electrical activity and summary table of procedures for electrical stimulation of the selected neural network. *(A) Illustrates the different time points when electrical recordings were done prior to any electrical stimulation. (B) This table gives a summary of the procedures carried out for the electrical stimulation experiment done on one neural network.*

4 .7 Data Analysis

In the Multichannel DataManager program, the file recordings were converted to Nexon system file format (NEX) and uploaded to Neuroexplorer, where the data was filtered using an in-house developed script. The script functioned to rename each electrode, as well as detect and filter the recorded LFP of the NEX multichannel files. Each LFP was registered as a single spike. Using the Neuroexplorer burst analysis program, the MFR and mean interspike interval (ISI) of each channel were calculated to return the results of the bursting profile of neurons recorded at each channel. Bursts were detected using the Poisson surprise method in Neuroexplorer. The algorithm identified episodes where series of spikes occurred with sequentially low ISIs (< MeanISI/2) at each electrode. The raw data from all Neuroexplorer analysis were exported to Excel and imported into MATLAB where the presented graphs were generated. To obtain the MFR at different timepoints during network development, the total number of spikes recorded at each electrode was divided by the total length of the recording (MFR = totalSpikes/length of recording). A sum was taken of all the mean spike/sec values at each electrode / number of recording electrodes (i.e.59) to produce an average MFR (avgMFR). Similarly, the sums of all the mean bursts/minute at each electrode / 59, were taken to produce the average mean burst rate (avgMBR) for each network at corresponding DIV.

For Network 2, the data generated from the Neuroexporer burst analysis for 44 DIV contained values that were 2 std above the mean for both the MFR and MBR. These outliers were detected and replaced with the avgMFR and avgMBR value for that period of recording respectively.

Furthermore, the file recordings were converted to a Hierarchical Data Format (HDF5), a format designed to organize and store large amounts of data and one supported by MATLAB. The MATLAB analysis toolbox, which is an interface for HDF5 files format created by Multichannel DataManager software, provided algorithms for systematically analyzing the HDF5 data. The toolbox was used to calculate the MFR for the spike data as well as produce simple raster plots to visually examine the spikes recorded at each electrode in the network. All results incorporated the electrodes at which no activity was recorded. Graphs and plots were further processed in Microsoft Paint, and Microsoft PowerPoint.

5. RESULTS

The results are summarized in four main sections; first, the healthy iPSC-derived NLS cells that were interfaced onto multi-electrodes arrays with an astrocyte substrate developed neurotypic markers similar to what is seen *in vivo*. Second, immunocytochemistry identified general neuronal markers such as beta-tubulin rich cytoskeleton, as well as more specialized cellular compartments such as pre-and post-synaptic areas and nicotinic acetylcholine receptors. Third, when synapses began to be established, *in vitro* neural networks had intrinsic properties such as self-emergent electrical excitability. There were also age-specific patterns of electrophysiological activities such as early primitive firing that later developed into complex patterns of network synchrony and bursting behaviour that could be seen across all networks. Finally, network perturbation by electrical stimulation suggested intrinsic neural network neuroplasticity.

5.1 Morphological observations of hiPSC- derived neural networks on MEAs

Most of the neural lineage cells that were seeded on surfaces without an astrocyte layer, showed increased detachment with floating aggregates, as well as prominent cell death by 7 DIV (Fig.9, B). Compromised cells were round, free-floating and uneven (Fig.9 B, red box) or attached but round and without neurite extensions, which are both indicators of dead and dying cells respectively. Furthermore, unhealthy cultures had cells with many stress vacuoles that were visualized as white/bright intracellular round spots usually around the nucleus on attached cells. Surviving cells in the unhealthy culture had a few, short neurites after 3 DIV however, this decreased drastically by 7 DIV. In contrast, neurons on astrocyte feeder layer surfaces had a healthier development assessed by observing neuron morphology and, neurite outgrowth. There was clear visibility of neuron soma (Fig.9 A, black arrows) as well as neurites that made connections with each other in the network (Fig.9 A, blue arrows). The somata of astrocytes were distinctly larger than those of neurons (Fig.9 A, yellow arrows) and we could see that the neurons grew on top of them. While cell survival can be determined using a number of assay protocols, in this case survival was visually assessed via light microscopy by noting the density of live attached neurons with neurites and the distribution of floating dead cells at times of media changes.

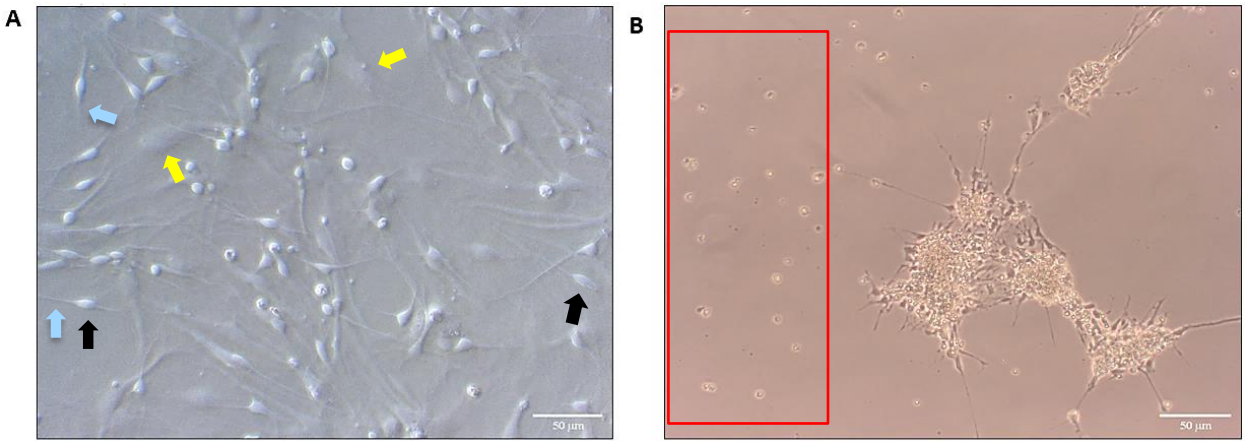

Figure 9. Phase contrast image of cultured neural lineage cells with (A) and without (B) astrocytes on coverslip at 7 DIV. *The hiPSC-derived neural lineage cells cultured with astrocytes showed more robust attachment at 7 DIV. Neuron cell body can be visualized (black arrows) as well as astrocytes cell bodies (yellow arrows). The blue arrows point to neurites. The latter culture (B) had fewer cells attached, many of which formed clusters. There were minimal neurite extensions with little or no connections with each other. The red box highlights an area of floating dead and/or dying cells. Scale bar, 50 µm. Magnification (A) 20X; (B)10X*

Likewise, on the MEAs with astrocytes, neurons achieved full confluence with dense networks around individual electrodes by 7 DIV (Fig. 10, A and B), with healthy attachment and survival persisting up to 60 DIV (Fig.11, C and D). Images A-D in Figures 10 and 11 represent snapshots from different timepoints during the development of the neural network, showing increasing complexity and interconnectedness. The snapshots were taken at different orientations on the MEA to give an overview of the organization of the neural networks. Similar to the coverslip images presented in Figure 9, presented, the somata of neurons and astrocytes were discernible (Fig.10 A, black and yellow arrows respectively). There also appeared to be differences in the size of neurites between 3 and 7 DIV, with the neurites at 7 DIV appearing thicker and more defined than those at 3 DIV indicating a more mature morphology. Finally, by 60 DIV the neurons had more pronounced arborization and we could observe distinct axon bundles growing together (fasciculation) and then separating (defasciculation) (Fig.11 D, blue arrows).

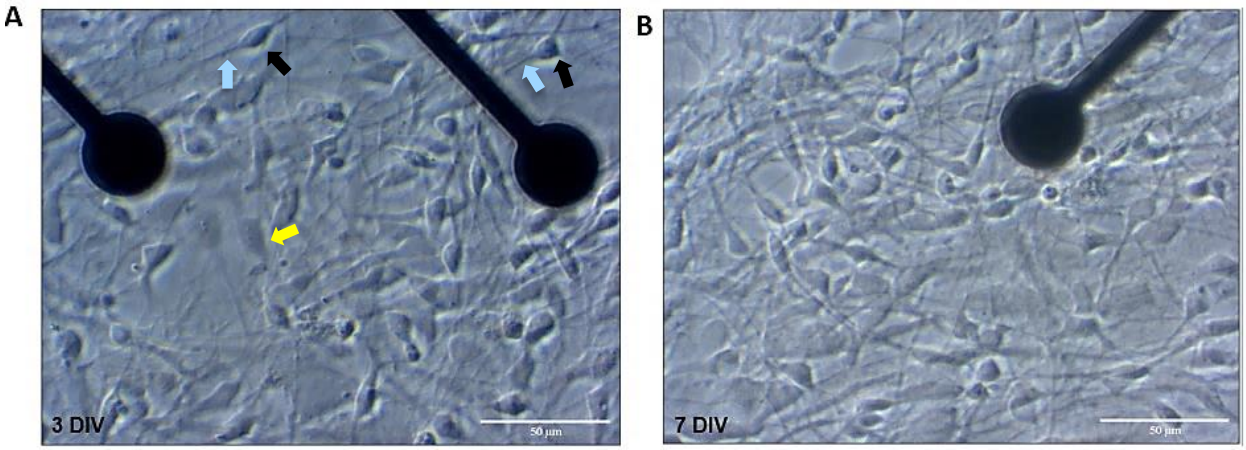

Figure 10. Phase contrast images of the cultured neural network on MEA. *A and B are representative images from one of the in vitro neural networks at 3 DIV and & 7 DIV respectively. The yellow arrows highlight the somata of astrocytes, black arrows highlight somata of neurons, and the blue arrows highlight the neurites. Scale bar, 50 µm. Magnification 20X.*

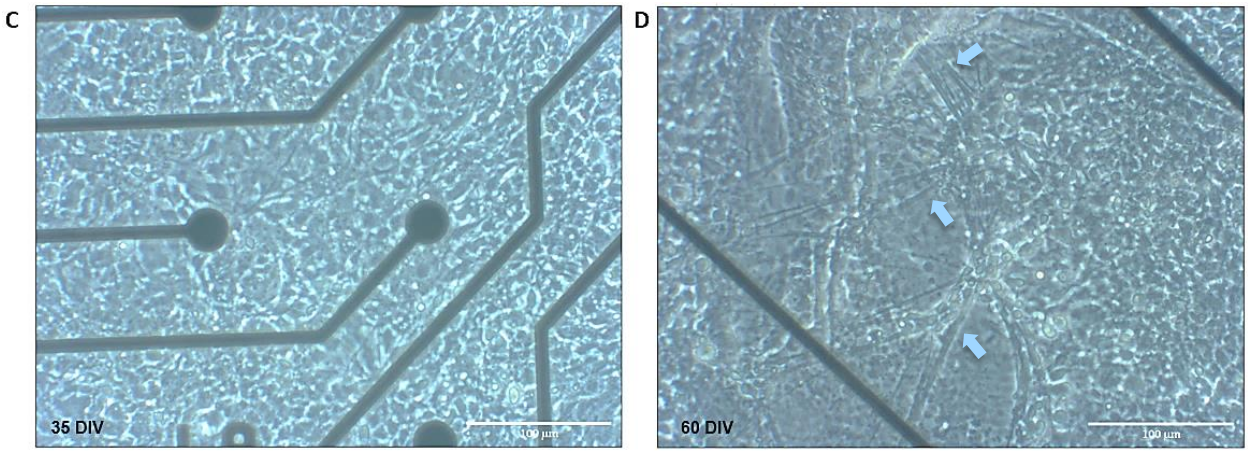

Figure 11. Phase contrast images of the culture neural network on MEA. *These images show the same network depicted above at 35 DIV (C) and 60 DIV (D). A comparison between the network at 3 DIV (Fig.10) and at 60 DIV shows an increase in complexity of the network. The blue arrows points to apparent fasciculated axon bundles. Scale bar, 100µm. Magnification 10X.*

5.2 Structural maturation of *in vitro* neural network

To assess the progression of neuronal maturation in the *in vitro* networks, we performed immunofluorescent labeling against several neuron-specific markers. Neuron specific microtubules were made visible by the beta III tubulin antibody (Fig.12, TUJ1). This highlighted a vast network of neurite extensions and arborization. It was also clear that many of these processes contacted each other. Moreover, the neural network had established presynaptic compartments (Fig.12, synaptophysin) that could be visually juxtaposed specifically along neurites.

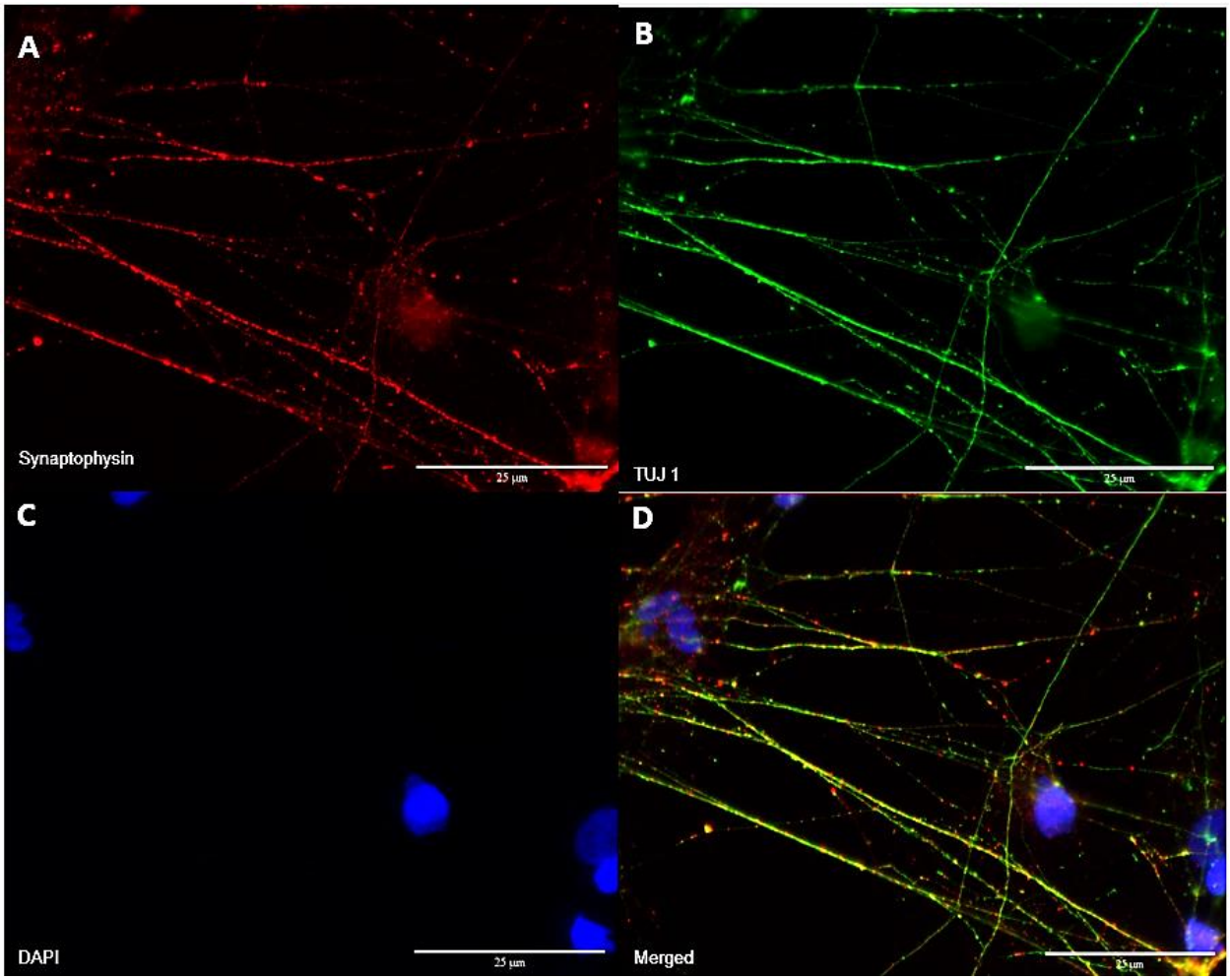

Figure 12. Representative neurotypic markers for maturing neurons. *Labeling to characterize synaptic development revealed prominent expression of the presynaptic marker, synaptophysin as well as neuron-specific protein (TUJ1). The image also incorporated a DAPI nuclei stain (4',6-diamidino-2-phyenylindole (DAPI), blue). Magnification, 100X. Scale bar, 25µm.*

Our results also suggested the development of both pre (synaptophysin) and post (PDS-95) synaptic assemblies (Fig.13), as well as indicated that the pre and post synaptic markers expressed were close to each other. The presence of astrocytes was also detected (Fig.13, GFAP)

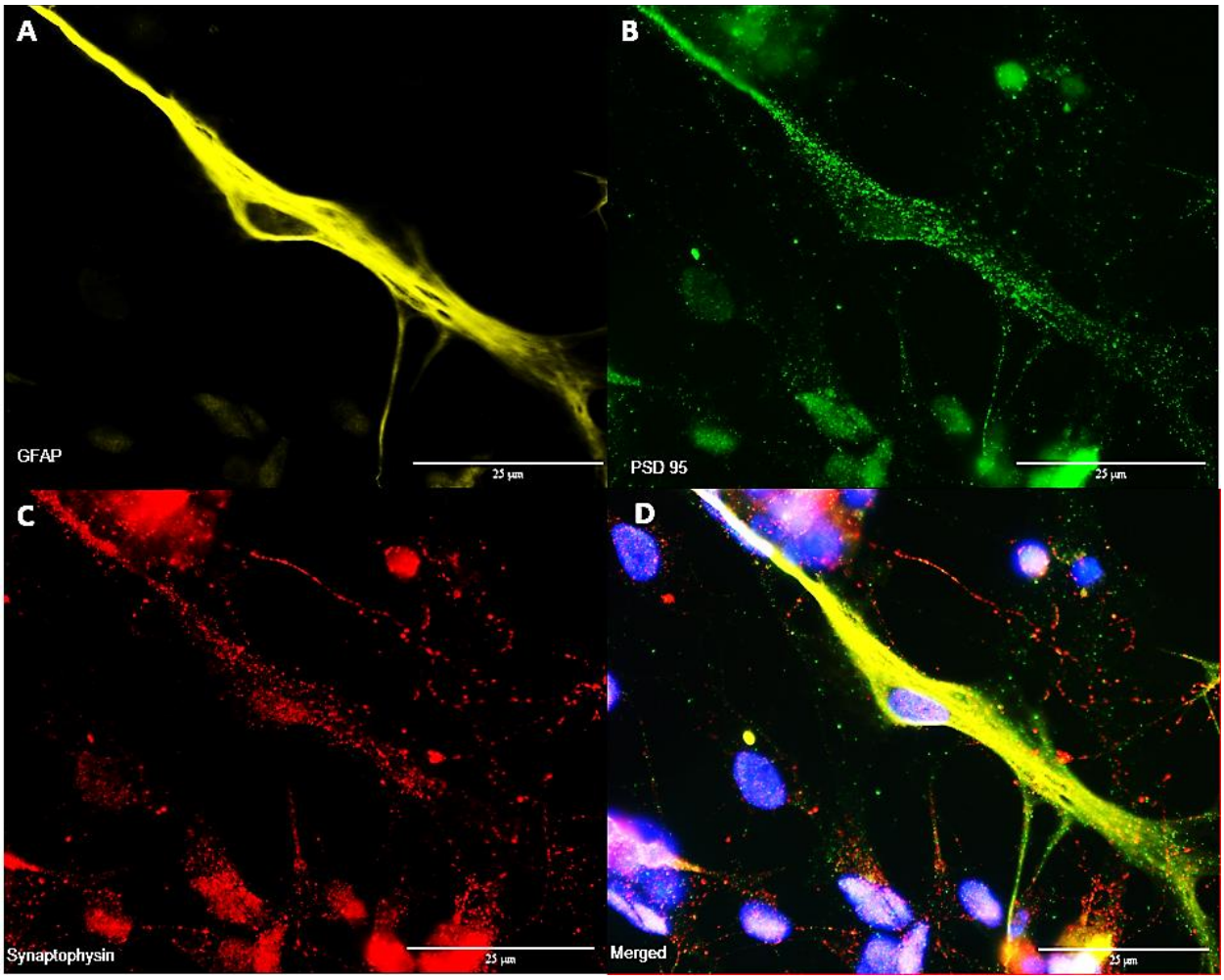

***Figure13*. Representation of synaptic areas in in vitro neural network.** *The image shows distributed presynaptic areas (synaptophysin) and post synaptic areas (PSD-95). Astrocytes were detected using GFAP. DAPI nucleic stain is visualized in blue. Magnification, 100X. Scale bar, 25µm*.

Finally, immunocytochemistry revealed the presence of post miotic cells in the neural network, based on the expression of the marker NeuN that labels differentiated neurons (Fig.14, NeuN). Furthermore, we were able to infer that cells (neurons and astrocytes) had extensive and complex cytoskeletons comprised of filamentous actin structures based on the very strong expression of phalloidin (Fig. 14). Actin filament is present in both astrocytes and neurons; therefore, it is difficult here to exactly distinguish neuronal processes from astrocytic ones. Finally, we also found that at 14 DIV, neurons were expressing specific receptor types due to prominent expression of nicotinic acetylcholine R a1 across the network.

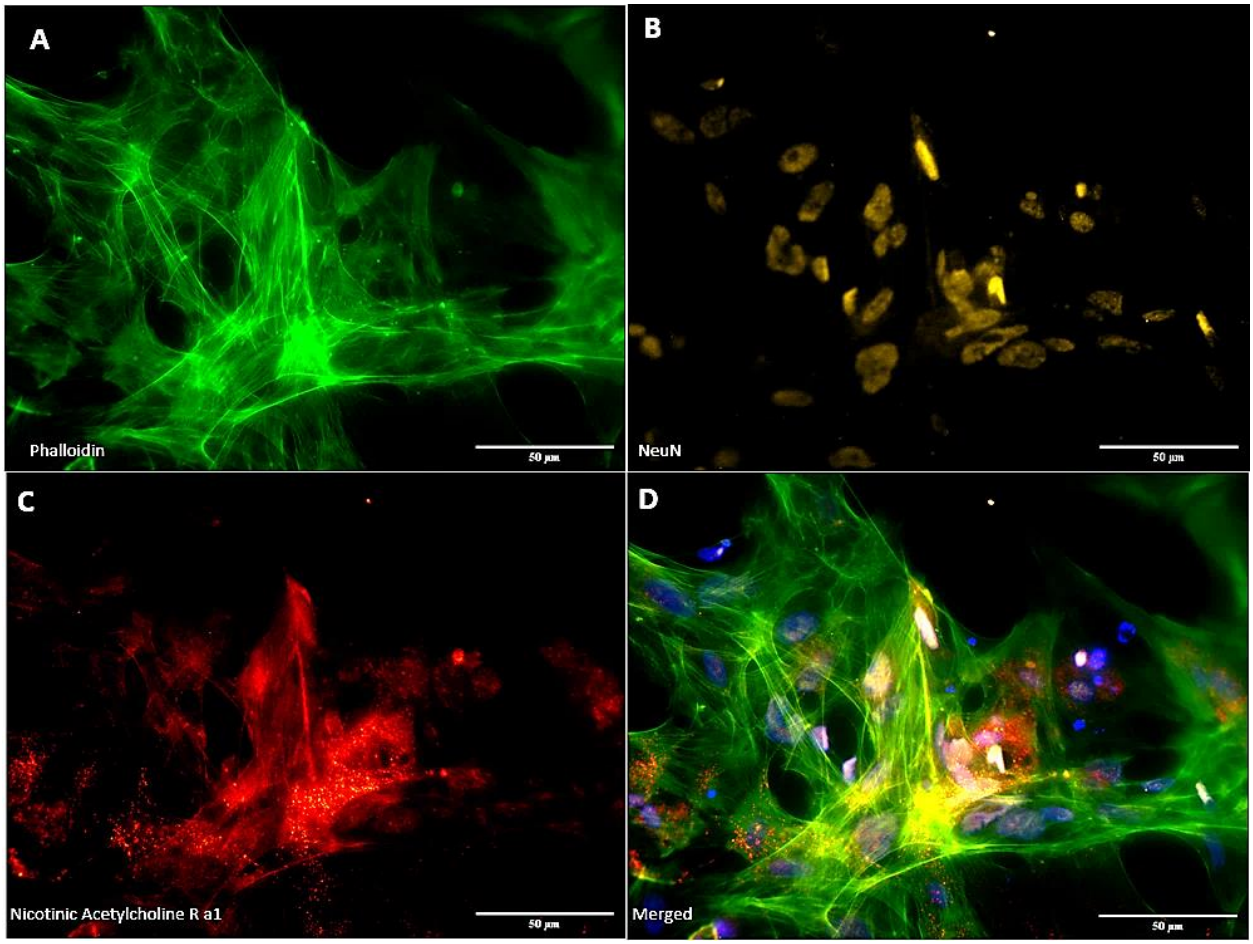

Figure14. Representation of cellular components. *The image shows extensive expression of the post mitotic marker NeuN (yellow). The red markers highlight nicotinic receptors and the strong expression of phalloidin (green) shows the abundance of actin filament in the network. The merged image incorporated a DAPI stain. Magnification 40X. Scale bar, 50µm.*

5.3 Development of spontaneous electrophysiological activity

There was an observable correlation between the development of the firing profile of the three neural networks and age. All three neural networks followed each other closely in average MFR development across the entire recording period. There was a prominent increase of >100% in firing rates between 09 DIV and 15 DIV (Fig. 15, B1). This increase in electrical activity remained relatively stable at a plateau for all networks until 28 DIV. Between 28 DIV and 35 DIV, there was a negative linear relationship between the firing rate and age for all cultures, which was succeeded by a peak at 40 DIV (Fig. 15, B2). The mean burst rate (MBR), however, where distinct for each network. At 09 DIV, only Network 3 had spikes that were registered as occurring in bursts, with avgMFR (spikes/sec) being 0.058 and the avgMBR (burst/min) being 0.021 (Table B1 and B2 respectively). However, at 15 DIV, the avgMBR was 0, while Networks 1 and 2 had started to develop a bursting profile. Post 18 DIV, all three neural networks exhibited increased bursting activity. Furthermore, the peak in firing activity at 40 DIV was followed by a steady decline that was maintained for all subsequent recordings for all networks. Finally, even though each network had its own unique electrophysiological qualities, the avgMFR did not differ notably (Fig. 16, B2), nevertheless there was a clear difference in the avgMBR, where Network 3 had consistently more bursts occurring in the spike trains.

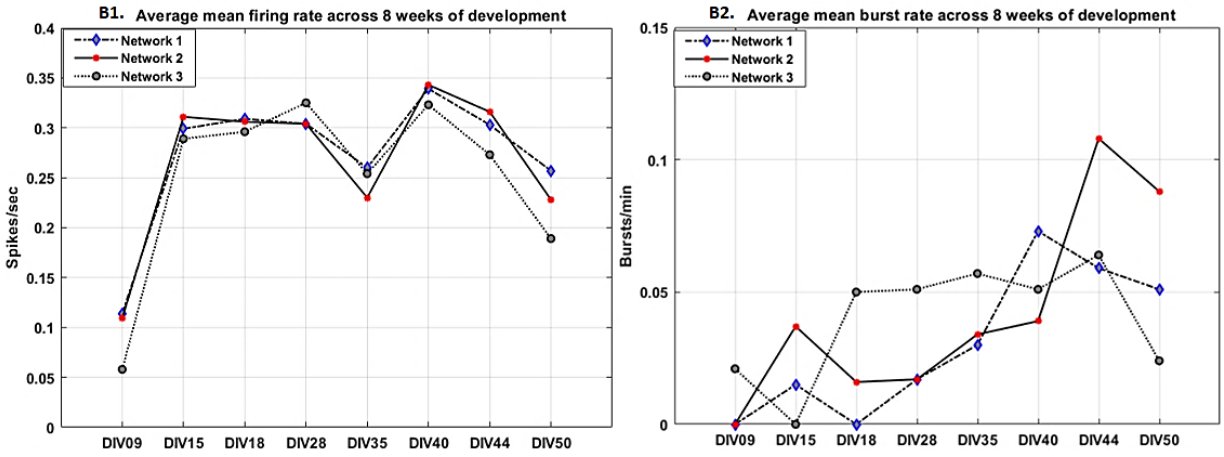

Figure 15. Average mean firing rate and average mean burst rate, respectively, at different timepoints across 8 weeks during the development of the in vitro neural networks.

The values for the avgMFR and avgMBR at each time of recording are listed in tables B1 and B2 and correspond to the line graphs presented in Figure 15. While it appeared that progressive bursting behaviour started at > 18 DIV for all neural networks, there was no trend among the three networks, as each developed its own unique level of activity (Table B2). There was, however, a general decline in the avgMBR for all networks that was also consistent with the decline in firing activity between 44 and 50 DIV for all networks (Fig.15). There were declines in burst rates from 0.06 to 0.051 for Network 1 and 0.11 to 0.088 for Network 2 (Table B2). Network 3 also had a decrease from 0.064 to 0.24 (bursts/min) between 44 and 50 DIV after having a relatively stable avgMBR between 28 and 40 DIV.

Table B1 and B2. Average mean firing rate and average mean burst rate respectively for each in vitro network, with the values corresponding to the line plots presented above for different time points during development.

B1. Average mean firing rate (spikes / second)

	NETWORK 1	NETWORK 2	NETWORK 3
DIV09	0.114	0.109	0.058
DIV15	0.299	0.311	0.289
DIV18	0.309	0.306	0.296
DIV28	0.304	0.304	0.325
DIV35	0.26	0.23	0.254
DIV40	0.339	0.343	0.323
DIV44	0.303	*0.316*	0.273
DIV50	0.257	0.228	0.189

B2. Average mean burst rate (bursts / minute)

	NETWORK 1	NETWORK 2	NETWORK 3
DIV09	0	0	0.021
DIV15	0.015	0.037	0
DIV18	0	0.016	0.05
DIV28	0.017	0.017	0.051
DIV35	0.03	0.034	0.057
DIV40	0.073	0.040	0.051
DIV44	0.06	*0.11*	0.064
DIV50	0.051	0.088	0.024

The raster plots of time series spikes (Fig.16) portray the activity of Network 3 across different timepoints during its development for approximately 60secs of recording. Periods of global activity were noticed occuring at most or all electrodes (blue vertical bars). These events appeared at periodic intervals with no reproducible spatio-temporal sequence. In addition, within this global synchronization, network bursts were observed at a few electrodes (yellow vertical bars) lasting for a duration of ± 1.5 seconds.
Other high frequency events were detected at individual electrodes for the duration of the recording period (red horizontal bars). There could be bursts events here, however, these may also be artifacts produced by signal drift.

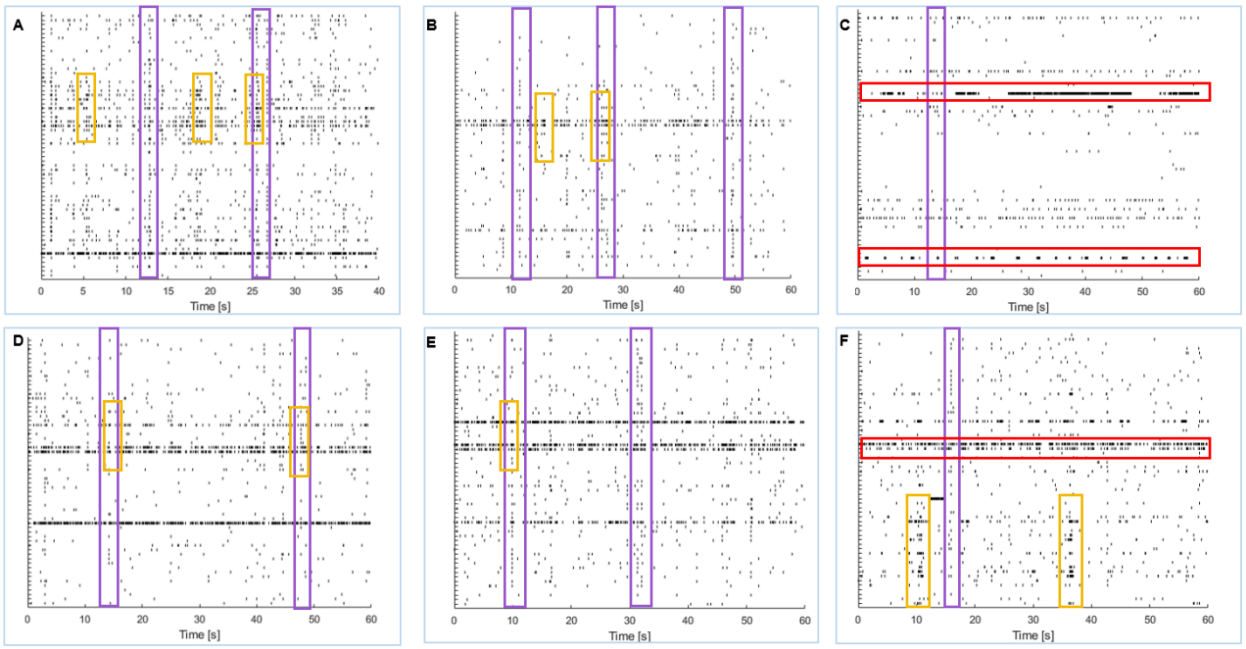

Figure 16. **Emergence of spontaneous synchronous electrical activity in one monitored in vitro neural network.** Recorded LFP (spike) is depicted as a single vertical line. *The horizontal ticks on the y-axis are the recording channels and each represent the spike train recording for one electrode. The darker areas where the spikes occurred together may be considered bursts. The blue vertical bars highlight periods of network synchronous activity across most or all electrodes. The yellow vertical bars highlight areas of synchronized bursts simultaneously occurring at a few electrodes, and the red horizontal bars show high frequency activity at single electrodes across the recording period. The x-axis is the time in seconds for the duration of the recording period (60 seconds of the total 3 minutes recording). (A) 09 DIV; (B) 15 DIV; (C) 28 DIV; (D) 40 DIV (E) 44 DIV; (F) 50 DIV*

5.4 In *vitro* neural network response to perturbation

The maximum MFR calculated at each electrode (EL) is presented for Network 3 at 57 DIV. The threshold of 20 (spikes/sec) is indicated by the color bar on the y2-axis (Fig.17). At 50 DIV, the presented neural network had 3 electrodes with MFR values > 15 spikes/sec (El_21 = 19.51; El_12 = 15.27; El_32 = 17.16). However, at 57 DIV, only one of the three electrodes had a MFR above 15 spikes/sec (El_32 = 31.89). Based on these results, El_21 and El_32 were selected for electrical stimulation in the sample network.

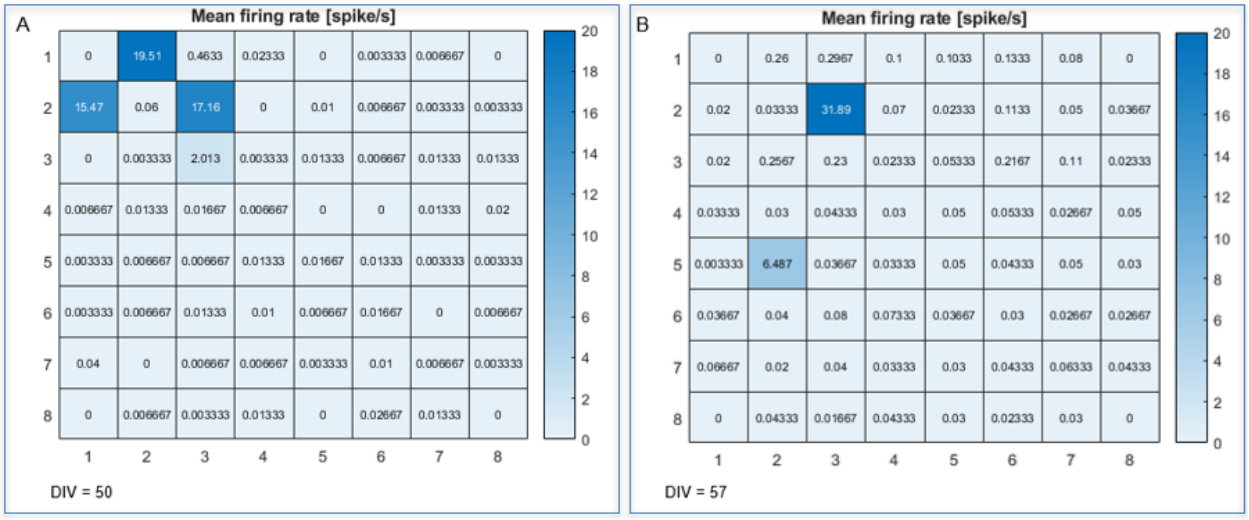

Figure 17. Mean firing rate (spikes / second) for one network (Network 3) at 50 and 57 DIV. *The graph represents the layout that follows the physical geometry of the MEA. Each square represents one electrode. The values on the x-axis (left to right 1-8) represent the columns, while the values on the y1-axis (top to bottom 1-8) represents the rows. Electrode numbers are read columns: rows and each panel within each graph represents an electrode (El_#). El_15 is the reference electrode. The color bar on the y2-axis shows the max value MFR at 20 (spikes/sec).*

Electrical activity was monitored both as spontaneous firing (pre stimulation) and as responses to the electrical stimulation (20 minutes and 24hrs post). The raster plot for the pre-stimulation recording revealed instances of global network synchronized activity, highlighted by the blue vertical bars in Figure.18 (A). The network synchronous activity appeared to occur at random intervals across the recording period (300 seconds). In addition, there was also distributed activity outside these global synchronized events, with two electrodes exhibiting high frequency activity for the entire recording period (Fig.18 A, yellow arrows). The electrodes for stimulation are highlighted by the blue arrows in Figure.18 B. At the onset of electrical stimulation, an artifact was observed at these stimulating electrodes producing the black horizontal line. Furthermore, the global activity noticed in (A) was disrupted during the electrical stimulation (B). The change in network activity persisted for the entire 600 seconds duration of the stimulation. The activity highlighted by the red and yellow horizontal bars (B) might be due to the neurons responding, however, these may also be artifacts created by the stimulation propagating through the culture media.

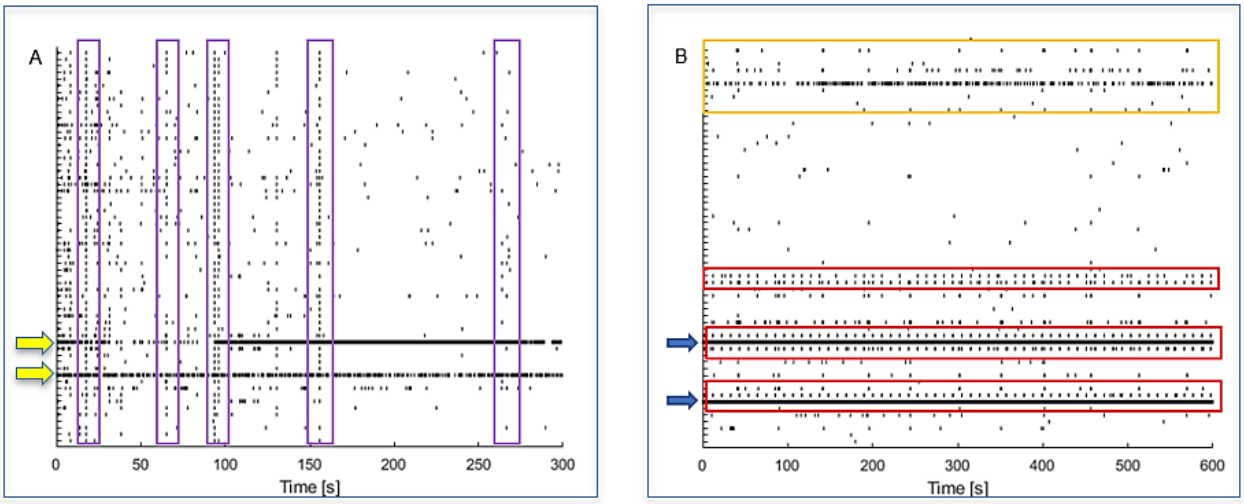

Figure 18. Raster plots of the network response to electrical stimulation applied at two electrodes*. The neural network had global synchronous events, at no defined time intervals (A, blue vertical bars). B) shows the activity for 600 seconds of electrical stimulation. The global network activity noticed in A was disrupted across the entire network. The yellow horizontal bar highlights increase activity at electrodes distal to the stimulating ones. The blue arrows (B) are the electrodes that have been stimulated (El_32 (top) & El_21 (bottom)).*

Recordings taken 20 minutes post stimulation (Fig.19, C) and at 24 hours post stimulation (Fig.19, D) showed a defined network response to the electrical stimulation. What was apparent was a restoration of the global synchronization as early as 20 mins post stimulation (Fig. 19). There was also a prominent decrease in activity post stimulation at the two electrodes that registered high frequency activity for the duration of the recording (Fig.18 A, yellow arrows). Furthermore, there was an overall increase in network activity in comparison to the pre-stimulation recording, with frequent occurrence of global synchronized events (blue vertical bars, Fig.19, C). Interestingly, while there was no distinct temporal pattern of global synchronization at 20 minutes post stimulation, the activity at 24hrs post stimulation revealed that most spikes occurred within global synchronizing events. These events unlike what was seen at 20 minutes post stimulation, had a defined temporal structure and occurred with intervals of ± 20 seconds (Fig.19 D, blue vertical bars). The synchronizing events for both conditions contained individual spikes outside global activity as well as what appeared to be distributed bursts at individual electrodes for the duration of the recording (green horizontal bars).

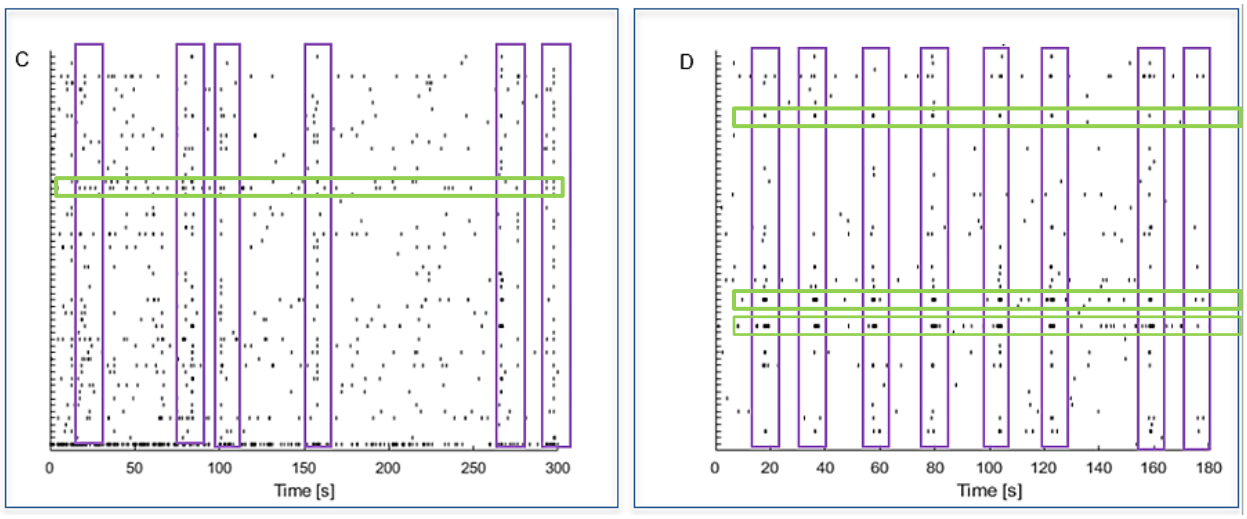

Figure 19. Raster plots of the spontaneous electrophysiological activity of the stimulated neural network at 20 minutes post stimulation (C) and 24 hours post stimulation (D). *Periods of restored global network synchronization were noticed for both conditions (blue vertical bars). The green horizontal bars highlight possible bursting across individual electrodes.*

The network activity recorded at each electrode 20 minutes post stimulation and 24 hrs post stimulation corresponding to each day are shown in Figure.20. There was an increase in the avgMFR from 0.269 spikes/sec) at pre-stimulation (baseline), to 0.355 (spikes/sec) 20 minutes post stimulation on Day 1. A further increase was noticed at 24hrs post (0.428 spikes/sec). The neural network activity 20 minutes post stimulation had a slight linear decrease in avgMFR across the 3 days of applying electrical stimulation (0.355, 0.343 and 0.324 spikes/sec respectively). On the other hand, the spontaneous activity 24hrs post stimulation had fluctuation across the 3 days. There was an increase in avgMFR from 0.428 to 0.456 (spikes/sec) at 24hrs and 48hrs respectively post the beginning of the stimulation period. However, a subsequent decrease to 0.312 (spikes/sec) was observed at 72hrs post the beginning of the stimulation period. Finally, these results confirmed that there was a consistent overall increase from baseline in the spontaneous electrophysiological activity in the neural network.

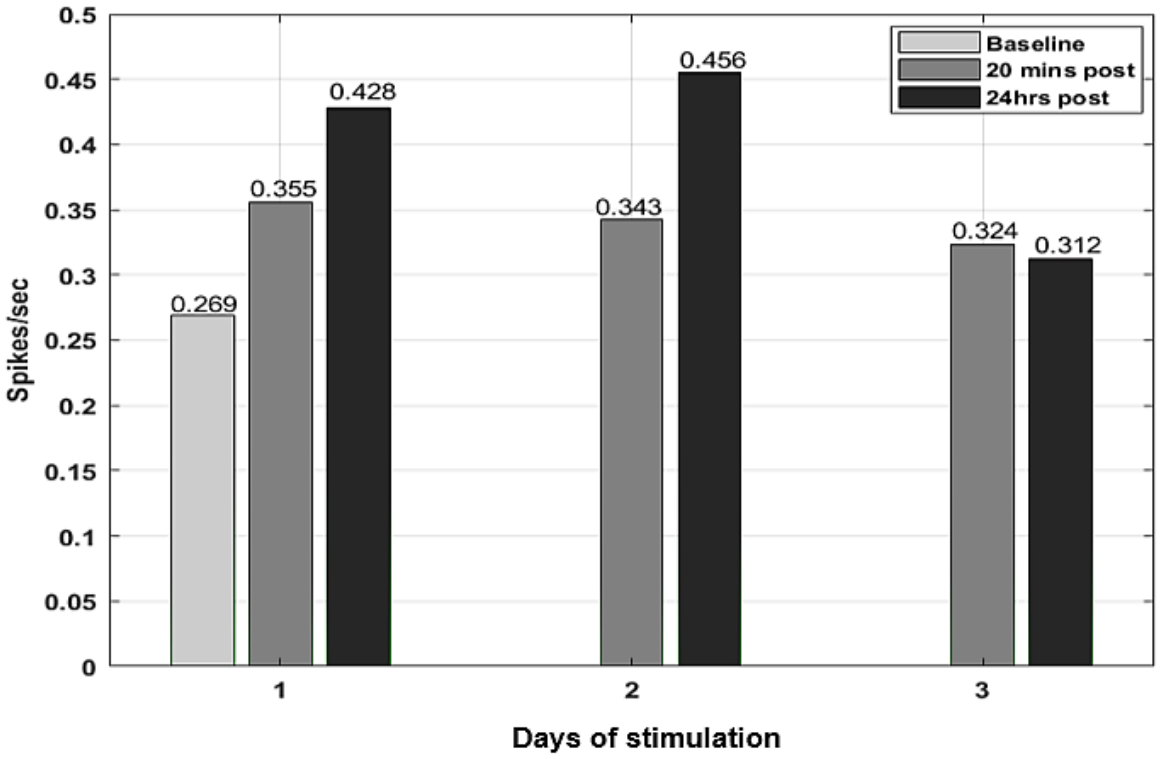

Figure 20. Bar graph of the average mean firing rate (avgMFR) for Network 3 during the stimulation protocol*. The bar graph shows an overall increase in activity from the baseline recording. The x-axis shows the 3 days of applying electrical stimulation. The legend describes three conditions for recordings: baseline, 20 minutes post stimulation and 24 hours post stimulation.*

The raster plots below highlight an overall decrease in activity across the network, as well as an eventual abolishment of global network synchrony. At 24hrs and 48hrs post the application of electrical stimulation, the *in vitro* neural network exhibited global network synchronization with ± 20 seconds intervals between each event (blue vertical bars, Fig.21, A and B respectively). There was also the occurrence of distributed activity outside these global events for both periods. In addition, some electrodes recorded what appeared to be persistent neuronal bursting behaviour for the duration of the recording for both periods (Fig.21, red horizontal bars). Finally, the 72hrs post stimulation recording, showed that the activity seemed to return to a stochastic state with repeated stimulation. We observed a total decrease in the electrophysiological activity across the network, as well as no distinct global synchronous events (Fig.21, C).

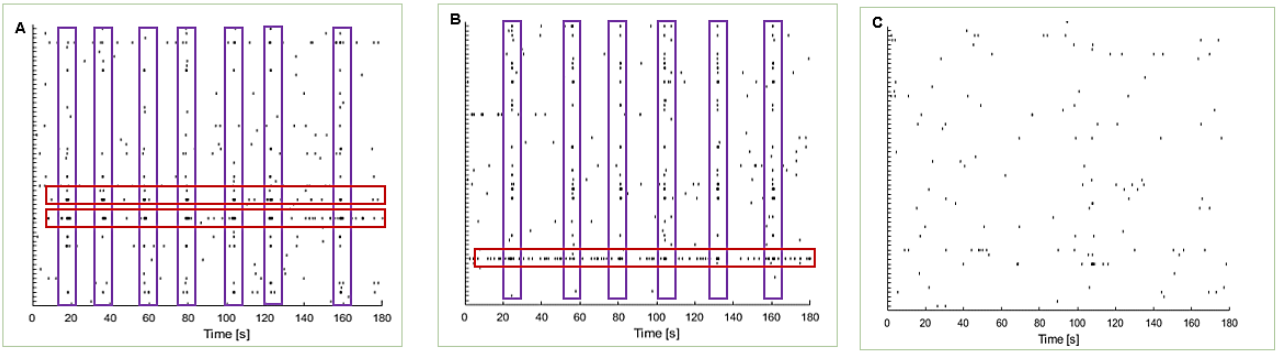

Figure 21. Raster plots showing the activity profile for the stimulated neural network at 24hrs post stimulation across the 3 days of electrical stimulation *(A) 24hrs post the application of electrical stimulation (Day 1); (B) 48hrs post the application of electrical stimulation (Day 2); (C) 72hrs post the application of electrical stimulation (Day 3). All 3 recordings were 180 seconds. The vertical blue bars highlight global synchronous events. The red horizontal bars highlight high frequency activity at individual electrodes.*

6. DISCUSSION

The primary aim of this master's thesis was to recapitulate *in vitro* structural and functional aspects of complex network dynamics of in vivo neural networks using hiPSC derived neurons. This entailed establishing viable hiPSC-derived neuron cultures, as well as monitoring the self-organization and evolving electrophysiological maturation of these networks using MEAs. Network perturbation through the application of electrical stimulation was also performed and the network responses were assessed. The main findings from the experiments are discussed in the following sections. These provide insights into the self-organization and emergence of spontaneous electrical activity, and network responses to stimulation, in the overall context of neuroplasticity.

6.1 Self-organization and emergence of structural complexity of hiPSC-derived neural networks *in vitro*

As previously mentioned, to model dynamic brain networks, a more physiologically relevant microenvironment can be achieved in vitro by the incorporation of astrocytes in the *in vitro* neuronal cultures [45,46]. As demonstrated in our results, visual inspection confirmed that co-culturing the neurons with astrocytes improved the survival and establishment of the neural networks when compared to monoculture (Fig.9). Importantly, monocultured neurons also had very few neurite projections, which made minimal to no contact with other neurons when compared to the extensive interconnectedness of the neurons co-cultured with astrocytes at the same time point post-seeding (Fig.9, B). Furthermore, it was directly visible on the MEAs (Fig.10&11) that the co-cultured *in vitro* neural networks matured beyond 50 DIV. Specifically, these neurons developed to form increasingly complex interconnected structures, with extensive neurite projections as well as what appeared to be fasciculated axon bundles (Fig.11). This is congruent with previous studies, making it possible to reason here that astrocytic role in facilitating synaptic connections within developing networks may be the major contributor to the increased neuron survival observed [45,46,49]. This is relevant since neuron survival is highly dependent on synaptic inputs with each other. This is an inherent feature of developing circuits in the CNS, where neurons actively seek out defined targets and compete with each other to form specific connections. Neurons that are successful in connecting with their targets are stabilized in the circuit (and thus their survival is increased) while unsuccessful neurons are pruned by programmed cell death (apoptosis). This process of finding target connections is guided by a variety of signaling pathways, a number of which are astrocyte-mediated [49]. Therefore, this further highlights that with the inclusion of astrocytes, a more physiologically relevant microenvironment can be achieved for maturing *in vitro* neural networks.

Another important aspect of assessing the development of the *in vitro* neural network was characterizing hiPSC differentiation into neurons and verifying neuronal maturation. Results from the

immunocytochemistry revealed mature neuron specific proteins in the neural network at 14 DIV, including expression of beta III tubulin (TUJ1) (Fig.12). The cytoskeleton of neurons is made up of tubulin rich microtubules (8 α- and 9 β-tubulin isotypes), which are crucial for maintaining neuronal cytoskeleton and basic architecture, as well as morphogenesis of axons and dendrites [105]. Therefore, successful TUJ1 labeling in the neural network provided evidence that the hiPSCs were differentiated into neurons with extensive projections of maturing neurites, which, in accordance with visual inspection on the MEA at 60 DIV (Fig.11), branched out of fasciculated axon bundles (Fig.12, TUJ1). This is an important observation, given that fasciculation ensures that developing neurons grow in the right direction for proper network formation, and neurons defasciculate to form more targeted connections within the neural network. This is crucial for communication within the network since signal transmission relies on these successful connections to be made so that the probability of forming a synaptic connection between neurons is increased.

We could also say that the neural network was developing necessary structures to facilitate synaptic activity based on the prominent expression of receptors (Fig.14, nicotinic acetylcholine R a1), the membrane protein synaptophysin that occurs in presynaptic vesicles, as well as the post synaptic density protein 95 (PSD-95) that functions to anchor synaptic proteins in the post synaptic neuron (Fig.12&13). Labelling of these synaptic areas was relevant because they are necessary structures for facilitating signal propagation within the network. As mentioned in the Introduction (section 2.2.1), communication in the neural network is facilitated by intercellular transmission. Specific to these identified structures, in chemical synapses, an action potential in the presynaptic neuron can cause neurotransmitter filled vesicles located in the presynaptic active zone to be released across the synaptic cleft, and bind to receptors on the partner post synaptic neuron in a highly complex and specialized area called the post synaptic density (PSD) [106]. Therefore, we can assert that the neurons in the *in vitro* network had developed structural components to receive and integrate signals as well as propagate information across the network due to the extensive neurite projections [107].

Another important finding was astrocytes that appeared to be positioned close to pre and post synaptic areas, as revealed by astrocyte-specific GFAP immunostaining (Fig.13). Astrocytes can play a critical role at the perisynaptic areas at early stages of neural network development. Their positions underscore the functional role of astrocytes in shaping *in vitro* neural networks, particularly with regards to synaptic formation and the maintenance of synaptic structures [48,104]. It has been shown that cholesterol production by glia cells enhanced synaptogenesis, while decreased availability of cholesterol limited synapse development [107]. Another study highlighted that astrocytes promoted the formation of functionally mature synapses in the CNS, whereas in the absence of astrocytes only a few functionally immature synapses were formed [51]. Considering that the sequence of differentiation for neural progenitor cells *in vitro* follows the same strict cascade found *in vivo* [108,109], previous *in vitro* studies

also highlighted that neural networks were functionally inefficient prior to gliogenesis. Specifically, analysis of the spontaneous postsynaptic currents *in vitro* revealed that glial cells potentiated the frequency and amplitude of excitatory synaptic activity in cocultures compared to the lower levels of synaptic activity in glial-free cultures [51,110]. Additionally, cocultures were more responsive to electrical stimulation than the glial-free cultures [111]. Finally, other studies have suggested that the perisynaptic astrocytes can mediate synchronous behaviours, including bursting in the neural network [111,112]. Thus, we can surmise that by helping the developing neurons to generate their synaptic connections and regulating synaptic activity towards electrophysiological maturity [53], astrocytes likely have a promotional effect on the electrophysiological development and maturity of the *in vitro* neural network by putatively contributing to synaptic plasticity. This could direct the development of *in vitro* networks to a state that mimics what is seen in developing brain networks [53].

6.2 Synaptogenesis and the evolution of spontaneous network activity in *in vitro* neural networks

The results of the immunolabeling provided evidence of neuronal maturation in the *in vitro* neural network and suggested that the neural network had developed pre and post synaptic structures. However, the implication here is that while hiPSC-derived neurons may exhibit a wide array of neurogenesis markers (including NeuN, TUJ, synaptophysin and PSD-95), this alone cannot account for synaptogenesis [113]. The synapse is a major functional element in neural assemblies that allows for information transfer between neurons. Network functionality is characterized by synaptogenesis which involves the differentiation and specialization of synaptic terminals, and which directs the formation of synaptic contacts. Therefore, along with confirming neurogenesis, it is imperative to also include measures for verifying the emergence of spontaneous network activity to support the notion of functional synaptogenesis [113].

We found that in the early stages of network development, i.e. between 9 DIV and 15 DIV, network activity increased steadily in avgMFR from < 0.15 to approximately 0.30 (spikes/sec) (Fig.15) across the entire network for all three monitored networks and did not show any significant increase or decrease from 15 DIV to 28 DIV. However, between 28 DIV and 35 DIV (Table B1), there was a decrease in the avgMFR in all three neural networks to < 0.26 (spikes/ sec). The result of increased firing in the earlier stages may be due to the presence of astrocytes during the period of neuronal differentiation and maturation, which may have fostered connections between appropriate synaptic targets, and promoted the maturity of these synapses as discussed in the previous sections. Although neural network activity is highly variable across identically prepared neuronal cultures and between recordings, a considerable number of studies have reported consistency in network progression from a silent state or primitive network behaviour [24,53] to a more stable state of increased activity. This is in accordance with our own findings. However, since these earlier studies did not incorporate astrocytes in the network, but rather

relied on the subsequent gliogenesis to take place in culture, a relatively silent state would support the idea that the synapses formed in the absence of glial cells were inefficient and thus, could only engage in minimal activity. In our study, neural lineage cells already had a rich layer of astrocytes to help with the formation of structural and functional synapses and may have also promoted neuron spiking abilities to foster network wiring. Thus, the networks could develop quicker than expected. Nonetheless, it is also possible that we may have missed the silent period in the network development considering that our recordings commenced at 9 DIV.

Notwithstanding the high level of activity in the earlier stages, the overall trajectory of the *in vitro* neural network's electrophysiological activity was relatively consistent with other findings [24], showing a peak in the avgMFR occurring in our networks around 15 DIV of approximately 0.30 (spikes/sec) for all networks (Table B1). Consistent with previous reports [24,55], this was followed by a plateau in the activity, which occurred between 15 and 28 DIV in our neural networks. Finally, there was a steady subsequent decrease from approximately 0.3 to < 0.2 for one network occurring from 40 DIV onwards (Table B1.) This plateau, followed by a general network activity decline, could be indicative of the neural network achieving a stable, optimal state. There are undoubtedly many possible explanations as to why this plateau and decline in activity occurred. We can reason that the dynamic interactions between excitatory and inhibitory neurons lead to stable, low firing rates [114]. This idea would further support that the neural network had developed specialized synapses (inhibitory and excitatory) that may determine the firing patterns and are thus necessary for maintaining firing rate equilibrium. Considering also that during this phase of our experiment the *in vitro* networks received no external input, settling in a stable state characterized by low activity may be the most advantageous for functionality in terms of information transmission. We can reason that homeostatic scaling would play a crucial role here to reduce network wide activity to both prevent the saturation of synapses that may occur if activity was persistently high and increase neuron specificity to respond to and integrate novel, physiologically relevant information [101]. In addition, homeostatic plasticity mechanisms may support the network's ability to form stronger recurrent excitation, which may appear as periodic bursts in an overall quiet network [12]. Together, this might increase the efficacy of the neural network to undergo subsequent Hebbian plasticity changes as neurons maintain their sensitivity to variable features of synaptic inputs.

The present study further noted increased synchronous neural network activity that progressed with age, as was found in other studies [56]. Based on our results, the *in vitro* neural networks showed patterns of collective spikes occurring across the network as was depicted in (Fig.16). Within many of these global synchronous events, there appeared to be distributed network bursts. Though "network bursts" remains a highly inconsistently defined term, the generally accepted concept is that a network burst is a period of successive firing preceded and followed by silent periods [115]. Accordingly, we observed these events occurring across multiple electrodes simultaneously lasting ±1.5 seconds. This feature has been widely

identified in several other studies [116-118], and likely reflects that both synchronized firing and synchronized network bursting events constitute characteristic features of developing cortical networks.

However, there are some spatial limitations of the raster plots presented (Fig.16, as well as, 18, 19 and 21) since they only depict the LFP recorded at each electrode. This means that the spike data of single neurons is not necessarily what is measured, but rather the sum of action potentials of N number of active neurons that contribute to the signal recorded at individual electrodes. Considering this, it is difficult to say whether one or more neurons are recorded across multiple electrodes. Nevertheless, while these results are not conclusive, we can make some inferences based on the observed synchronizing events. Prior studies that have noted the importance of these synchronous burst patterns reported that they may play a function in propagating synapses in a directed manner and thus, facilitate the reliability of communication to strengthen synaptic connections in the neuronal network [68,119]. Since these synchronized bursts appeared on a global scale (Fig.16), we can surmise that there was a form of Hebbian functional synaptic correlation between neurons to facilitate synaptic strengthening necessary for this. Furthermore, we found that synchronized bursts were related to the different developmental stages of the *in vitro* neural network. One study reported that fewer spikes were distributed in synchronized bursts in the early stages < 8 DIV of network development, with lower firing rates, compared to more spikes observed at later stages > 15 DIV, with higher firing rates [120]. This comparison can also be made with our results showing that with age, more bursts were recorded in the neuronal network, relative to the linear increase in firing rates (Fig.15, B1 & B2; Table B1 & B2). It is also relevant to note that with age, synapses within the neural network would become more functionally mature, and thus, more effective at facilitating the propagation of more synchronized bursts. Furthermore, the wide variability in neural network activity can be highlighted by a comparison between the spiking and bursting profiles of the networks (Fig. 15, B1 & B2 respectively). Even though we observed a distinct course of activity in the avgMFR, there was no correlation in the avgMBR taken at the same time points for each neural network. From this, we can infer that while there is a general pattern of neural network development, each network still retained its own distinctly unique quality in the context of signal propagation.

Taken together, the results from immunolabeling and the spontaneous electrophysiological activity of *the in vitro* neural networks suggest that the hiPSC-derived NLCs differentiated into neurons on the MEAs and were able to self-organize into complex networks that could spontaneously form synaptic connections, likely indicating both neuronal maturity and structural and functional synaptogenesis. Furthermore, the resulting *in vitro* neural networks progressed through stages of electrical activity development that were reminiscent of those found in the *in vivo* context (namely, from primitive early activity of random spikes, to more complex patterns of network synchronization and bursts), thus depicting relevant features of developing neural networks. The capability of the *in vitro* network to self-

modulate its activity as an indication of intrinsic neural plasticity and adaptability mechanisms will be addressed in the next section.

6.3 *In vitro* neural network response to electrical stimulation

The effects of the electrical stimulation could be observed both as a temporary disruption in the global neural network synchrony, and as an overall activity increase at individual electrodes throughout the network (Fig.18). However, it should be noted that the measurements taken at the timepoint during stimulation may simply reflect the stimulation pulse (effectively an artifact) and not the network response to it. To more clearly evaluate the network response to stimulations, it was important to make recordings of the spontaneous activity at different times post stimulation. Interestingly, at 20 minutes post stimulation and at 24 hours post stimulation (Fig.19) network-wide synchronized firing and bursting were largely restored with possibly stimulus-induced modification in areas distal from the local stimulation point. This might suggest that activity-dependent plasticity in the *in vitro* neural network was not restricted to the projection of neurons proximal to the stimulation site, but rather likely depended on the initiation and propagation of the stimulus induced activity to cause a global network activity reorganization [69]. Furthermore, in the context of Hebbian plasticity, activity-dependent plasticity is favored by the Hebbian conjuncture of high presynaptic stimulation inducing postsynaptic excitation, in which case, the propagation of synchronized bursts from the local stimulation point to distal parts of the network would serve particularly to strengthen connections whilst conveying information about the nature of the stimulus [69].

While the activity at 20 minutes post stimulation had instances of global network synchronization (Fig.19 C, blue vertical bars), the activity was not distinctly reflective of the induced stimulation in the context of temporal structure. However, it was apparent that during the period between the 20 minutes post stimulation and 24hrs post stimulation, the neural network refined its activity such that more activity occurred within global synchronous events at approximately ± 20 seconds intervals (Fig. 19, D). Also, due to the observation of altered activity at distal electrodes, where the activity seemed to follow the timed pattern of stimulation, we may stipulate that the information content of the *in vitro* network i.e. the detection of the stimulus and possibly subsequent encoding, may be carried in the timing of these propagating bursts [121]. Although the stimulation pulse was set to ±10 second intervals, the resulting activity was scaled down and refined to bursts with distinct ±20 sec intervals, 24 hours post stimulation. This could be an indication that intrinsic neuron/network properties were employed to encode the electrical stimulus and ultimately refine the specificity of connections to produce the defined output behaviour, lending merit to the involvement of Hebbian plasticity mechanisms.

6.4. Did stimulation result in Hebbian activity-dependent modification of synaptic plasticity?

In the context of Hebbian LTP, the electrophysiological measurements were interpreted with focus on the persistence of the stimulus induced response that was observed 24hrs post stimulation in the *in vitro* neural network. However, it must be emphasized that other frames of interpretation may also apply. Accordingly, there was a distinct pattern of global activity that persisted up to 48hrs after the first electrical stimulation (Fig.21, A & B respectively). This activity could be a direct result of the electrical stimulation. Evidence to support this comes from the pioneering study conducted by Bliss and Lomo in 1973 where LTP was induced by repetitive stimulation and lasted several hours in the dentate area of the rabbit hippocampus [4]. Since this study, LTP persistence across protocols and brain areas has been widely categorized to lasting anywhere between some hours to several weeks, suggesting that the capacity for maintenance and subsequent decay are regulated by complex mechanisms that occur during the application of electrical stimulation, and preceding and following LTP establishment [122]. The endurance of network changes beyond 24hrs in our stimulated network, provided evidence for activity-dependent synaptic plasticity and suggests that the *in vitro* neural network had inherent competence to modify its activity after perturbation.

A pertinent question remains as to whether plasticity modification and persistence is enough to assume learning and memory. Considering that the *in vitro* neural network is incapable of exhibiting a behaviour akin to relevant behavioural output of animals in the *in vivo* context, we needed to examine the nature of the spontaneous activity 24hrs post stimulation. It is likely that the pattern of synchronized activity that was observed in our network 24hrs post stimulation may provide a descriptive indication of the functional mechanisms involved in the stable transfer of information in the network [123]. As pointed out earlier, neuronal activity can be quite variable between recordings and oftentimes, leading to problems with generalizability. As we could see in previous recordings of spontaneous electrophysiological behaviour where global synchrony was observed (Fig.16), there was no consistent temporal structure to synchronized events. However, the distinct temporal structure of the spike activity, i.e. the spontaneous synchronized activity of ± 20 second interval (Fig.21, A & B), strongly suggests that the stimulus/information was probably learned and thus, encoded and effectively propagated in the *in vitro* neural network. Also, it must be noted that the electrical stimulus should have directly affected only those neurons near the two selected electrodes to which it was applied and not the entire network. This would be the case especially in a dense network if there are neurons directly on top of the stimulated electrodes. The neurons would create tissue resistance to contain the stimulation to the localize area i.e. preventing it from spreading. Therefore, because the post stimulation synchrony was a network wide event and not just locally reserved to the areas proximal to the stimulation site, the results may imply an increased efficacy of synaptic connections between the synchronized neurons and indicated a functionally

interconnected network. This specificity of a patterned behaviour exhibited hours after the stimulation suggests that the *in vitro* neural network could produce a response.

Interestingly, if LTP can be restored to the original level with repeated high frequency stimulation [122], then the results of the network reverting to a stochastic firing behavior with gradually decreased spikes after 72hrs (Fig.21, C) was surprising. This result of decreased activity post repeated electrical stimulation made it important to reiterate that both LTP and LTD are probable results of the same process and the susceptibility of the *in vitro* neural network synaptic changes favoring either is still an area of intense research [124]. It is conceivable that during applied stimulation, some connections might be potentiated but others might also become depressed. Based on this, one possible explanation for the observed activity decline would be synaptic depression. However, to determine this, the exact dynamics taking place at pre and post synaptic areas would have to be examined, since this interaction constitutes the overarching idea of Hebbian plasticity. Effective coupling (and hence strengthening) of synapses relies on the successful binding of presynaptic neurotransmitters to relevant postsynaptic receptors. However, several reports asserted that presynaptic vesicles are a limited resource and their depletion in the presynaptic terminal may be a main cause of post synaptic depression during persistent activity [125]. This could provide some explanation of our results if we assume that the neural network organization on the MEA remained fixed and the same electrodes recorded the summed action potentials of the same neurons throughout the period of electrical stimulation and afterwards. This could signify that the same correlated neurons may be persistently activated during the period of electrical stimulation and post stimulation. Therefore, applying electrical stimulation to the same electrodes should cause activity to propagate in the same way each time, i.e. via the same correlated neurons. Based on this hypothesis, depletion would be likely at these synaptic areas. Evidence for this comes from our comparison of the 24hrs post responses for the three consecutive days (Fig.20) we notice that there was a gradual decay in potentiation.

As an alternative explanation, homeostatic mechanisms that work in tandem with Hebbian potentiation, may act to downregulate the functional availability of excitatory glutamate-type receptors on post-synaptic neurons [90] and overall, augment Hebbian plasticity in order to maintain synaptic homeostasis. The presynaptic neurons may also simply decrease the release probability of vesicles to allow the excitable neurons in the network to maintain their activity within a dynamic range to ensure normal propagation of activity through the neuronal network [90]. The instance of the activity-dependent LTP modification observed at 24hrs (Fig.21, A) would render connected synapses more excitable and reduce the threshold for further LTP in the same connections [126]. Thus, further stimulation to the same interconnected neurons would trigger homeostatic mechanisms operating as a negative feedback process, to prevent runaway excitation and gradually return the neuronal network to a highly desirable controlled state [93,98], as outlined in the Introduction (Fig.3). Therefore, the gradually reduced activity between 24hrs

and 48hrs post stimulations, and between the two former and 72hrs post stimulation (Fig.21, A, B, C respectively), could be due to intrinsic homeostatic downscaling of activity. It is also relevant to apply this conjecture to the down-scaling of the post stimulation spontaneous activity (from ±10 seconds interval bursts to ± 20 seconds interval bursts). This may have been a mechanism for conserving resources in the *in vitro* neural network. Also, it could mean that global burst of ±10 seconds intervals would cause the neural network to be too excitable or saturate synapses, both of which are unfavorable outcomes for the neural network and are risk factors for neural circuit pathology.

Although only one neural network was perturbed, thus reducing the generalizability of our results, we observed interesting indication of non-Hebbian robustness. This is an inherent feature of all known biological network systems and describes the system's capacity to maintain optimal functionality in the face of perturbation and uncertainty [16,127]. Unlike homeostatic plasticity, which is concerned with maintaining the state of the system (stability), robustness is concerned with maintaining system functionality [15]. However, there are converging elements in these processes such that homeostasis and stability may also be considered instances of robustness [15]. In this context, if we consider the baseline recording of the *in vitro* neural network, (Fig.18, A) to be the steady state of the network, characterized by synchronized global activity, then accordingly, electrical stimulation disrupts this state (Fig.18, B). Intuitively, disruption could leave the network vulnerable to pathology if it was unable to derive a new functionally steady state, adhering to the concept of inherent robustness. However, our results showed that the network could return to a new state that also indicated that functionality was maintained post perturbation. The *in vitro* neural network could restore global synchrony as quickly as 20 minutes post stimulation (Fig.19 C). Interestingly, we can also imagine that during the period of refinement between the 20 minutes post stimulation, and the 24hrs post stimulation (Fig.19 C, D), the *in vitro* neural network had the inherent capacity to continually derive multiple steady states to finally arrive at the activity-dependent modification. Furthermore, we can also stipulate that while in these new steady states, the *in vitro* neural system could maintain functionality. This is based on the distinctive temporal global synchronous activity noted post electrical stimulation, that indicated that information was being integrated and propagated throughout the *in vitro* neural network. Of course, this topic needs further study to arrive at a conclusive explanation. In that sense, this would be very interesting to explore in the future.

7. CONCLUSION

The overall aim of this master's thesis was to recapitulate intrinsic structural and functional dynamics of *in vitro* neural networks, such as self-organization and spontaneous synchronous network firing and burst patterns and provide insights as to how direct perturbation can influence network activity towards malfunction or adaptive learning states. We have shown through immunoassays and electrophysiological measures using MEAs that hiPSC-derived neurons demonstrate relevant behaviours comparable to those of *in vivo* neural networks based on inherent -emergent network properties.

We identified that consistent across all monitored networks were defined patterns of electrophysiological behaviour that were distinct at different points of network development. Interestingly, we found that all networks had starkly similar stereotypical pattern of increased primitive activity in the early stages, with a subsequent phase of refinement characterized by complex global synchronized events and network bursts that decreased over time. However, the inherent bursting behaviour for each network was random and completely unique between networks, highlighting that even though neural networks progress through these stages of electrophysiological maturity, they are still wholly different from each other. Furthermore, we showed that network perturbation by the application of electrical stimulation resulted in a disruption of the endogenous global synchronization in the network. Specifically, the *in vitro* neural network demonstrated a degree of adaptability by subsequent restoration of synchronous behaviour as early as 20 minutes post perturbation, with a stimulation induced temporal structure that persisted up to 48hrs. This provided strong evidence for both activity dependent Hebbian potentiation in the network as well as compensatory homeostatic which were discussed in the context of our results. Most importantly, it has raised interesting questions about how neural networks transition between stages of activity, such as ordered *versus* less ordered states, and maintain their functionality. We imagine that the road to providing answers to these questions is paved with exciting research perspectives.

8. LIMITATIONS

One major limitation of this study was the number of trials conducted and the small population of networks from which the results were derived. Since the inferences made in this research work were all based on the results obtained in the pilot test of the outlined hypotheses, it is appropriate to consider the reliability of the quantitative data. Initially we designed this study to be repeated with a larger number of neural networks, however due to time constraints this could not be completed. Therefore, we have strong intentions of expanding this study in the future.

Secondly, while there are many advantages of using the standard MEAs, they still have their limitations. Specifically, standard MEAs have limited spatial resolution so they typically do not allow for targeted recording from individual neurons so the information may not accurately reflect the activity of the network. Furthermore, due to high variance in the electrophysiological activity that was recorded, both between recordings and among electrodes, it was difficult to apply statistical analysis to the results. This is a matter of further development in the lab.

In terms of changes to the methods should this study be repeated; I would prefer to make recordings of the different developmental stages at defined intervals e.g. the same day and time every week. This may give a better comparability between the different points in the neural network development. In addition, performing immunoassay at different stages to note morphological changes in neurite size or synaptic densities for example, would provide stronger results of network morphology.

Finally, in the context of neural network response to electrical stimulation, I would include different populations such as networks that received longer/shorter stimulations or more/less repetition of stimulation. This would enable better comparisons about potential network adaptive or maladaptive response to different degrees of perturbations.

9. FUTURE PERSPECTIVES AND RESEARCH

This research work was a promising start to exploring the dynamics of healthy and perturbed *in vitro* neural networks. However, the most interesting part of the research to realizing a dream of understanding how *in vitro* neural networks interact with their designed world is still ahead. Contributions to these questions can be addressed in the short term and long term.

Short-term perspectives include a series of studies geared at elucidating structural and functional consequences of modulation of *in vitro* neural network activity using chemogenetic tools (Appendix 1 & 2). In addition to being compatible with electrical stimulations, MEA platforms can also be combined with such tools to help understand how molecular interactions and neuronal signaling specify normal and pathological neural network functions [41-43]. In general, hiPSCs-derived neurons can be transfected with chemogenetically engineered proteins such as Designer Receptors Exclusively Activated by Designer Drugs (DREADDs) (e.g. excitatory - *Gq* or inhibitory - *Gi*). DREADDs allow for transient and repeatable enhancement or silencing of synaptic activity in transfected neurons upon application of inert exogeneous ligands such as clozapine-N-oxide (CNO) [128,129]. Studies have found that chronic inhibition or disinhibition in a neural network results in distinct structural outcomes that affect spatio-temporal formation of neural networks and synaptogenesis [130,131]. This implies great potential for drug screening and discovery in the field of neural research [132].

In the overall long-term, it is relevant to provide a useful characterization of what a “stable” network state looks like and the degree of perturbation required to disrupt this state to malfunction. However, there are several conceptual and methodological challenges to overcome, in order to adequately interpret electrophysiological data derived from network recordings. Therefore, it is of great importance to develop reproducible models of network activity, which thereafter, can be used to answer questions of network pathology in disease models such as Parkinson’s, Alzheimer’s and epilepsy.

10. REFERENCES

1. Von Bernhardi R, Bernhardi LE, Eugenin J. What is neural plasticity? *Adv Exp Med Biol.* 2017; 1015: 1-15.

2. Fauth M, Tetzlaff C. Opposing effects of neuronal activity on structural plasticity. *Front Neuroanat.* 2016; 10(75).

3. Hebb DO. The organization of behavior: a neurophysiological theory. 1949. New York. Wiley.

4. Bliss TV, Lomo T. Long lasting potentiation of synaptic transmission in the dentate area of the anaesthetized rabbit following stimulation of the perforant path. *J Physiol.* 2973; 232(2):331-56.

5. Massobrio P, Tessadori J, Chiappalone M, Ghirardi M. *In vitro* studies of neuronal networks and synaptic plasticity in invertebrates and in mammals using multielectrode arrays. *Neural Plast.* 2015; 2015: 196195.

6. Matsuzaki M, Honkura N, Ellis-Davies GC, Kasai H. Structural basis of long term potentiation in single dendritic spines. *Nature.* 2004; 429(6993):761-6.

7. Lisman J, Yasuda R, Raghavachari S. Mechanisms of CaMKII action in long term potentiation. *Nat Rev Neurosci.* 2012; 13(3):169-82.

8. Barria A, Malinow R. NMDA receptor subunit composition controls synaptic plasticity by regulating binding to CaMKII. *Neuron.* 2005; 48(2):289-301.

9. Halt AR, Dallapiazza RF, Zhou Y, Stein, IS, Qian H, Juntti S, Wojcik S, Brose N, Silva AJ, Hell JW. CaMKII binding to GluN2B is critical during memory consolidation. *Embo j.* 2012; 31(5):1203-16.

10. Zhou Y, Takahashi E, Li W, Halt A, Wiltgen B, Ehninger D, Li GD, Hell JW, Kennedy MB, Silva AJ. Interactions between the NR2B receptor and the CaMKII modulate synaptic plasticity and spatial learning. *J Neurosci.* 2007; 27(50):13843-53.

11. Luscher C, Malenka RC. NMDA receptor-dependent long-term potentiation and long-term depression (LTP/LTD). *Cold Spring Harb Perspect Biol.* 2012; 4(6).

12. Abbott LF, Nelson SB. Synaptic plasticity: taming the beast. *Nat Neurosci.* 2000; 3 Suppl: 1178-83.

13. Perez-Otano I, Ehlers MD. Homeostatic plasticity and NMDA receptor trafficking. *Trends Neurosci.* 2005; 28(5):229-38.

14. Turrigiano GG, Leslie KR, Desai NS, Rutherford LC, Nelson SB. Activity-dependent scaling of quantal amplitude in neocortical neurons. *Nature.* 1998; 391(6670):892-6.

15. Kitano H. Towards a theory of biological robustness. *Mol Syst Biol.* 2007; 3. Pp.137.

16. Stelling J, Sauer U, Szallasi Z, Doyle FJ, 3rd Doyle J. Robustness of cellular functions. *Cell.* 2004; 118(6):675-85.

17. Leone DP, Srinivasan K, Chen B, Alcamo E, McConnell SK. The determination of projection neuron identity in the developing cerebral cortex. *Curr Opin Neurobiol.* 2008; 18(1):28-35.

18. McConnell SK, Kaznowski CE. Cell cycle dependence of laminar determination in developing neocortex. *Science.* 1991; 254(5029):282-5.

19. Frantz GD, McConnell SK. Restriction of late cerebral cortical progenitors to an upper-layer fate. *Neuron.* 1996; 17(1):55-61.

20. Desai AR, McConnell SK. Progressive restriction in fate potential by neural progenitors during cerebral cortical development. *Development.* 2000; 127(13):2863-72.

21. Noctor SC, Martinez-Cerdeno V, Ivic L, Kriegstein AR. Cortical neurons arise in symmetric and asymmetric division zones and migrate through specific phases. *Nat Neuroscience.* 2004; 7(2):136-44.

22. Pilaz, L and Silver DL. Post-transcriptional regulation in corticogenesis: how RNA-binding proteins help build the brain. *Wiley Interdiscip Rev RNA. 2015;* 6 (5): 501-15.

23. Kirwan P, Turner-Bridger B, Peter M, Momoh A, Arambepola D, Robinson HP, Livesey FJ. Development and function of human cerebral cortex neural networks from pluripotent stem cells in vitro. *Development.* 2015; 142(18):3178-87.

24. Chiappalone M, Bove M, Vato A, Tedesco M, Martinoia S. Dissociated cortical networks show spontaneously correlated activity patterns during *in vitro* development. *Brain Research.* 2006; 1093(1):41-83.

25. Gage FH. Neurogenesis in the adult brain. *JNeurosci.* 2002; 22(3):612-613.

26. Bond AM, Ming G, Song H. Adult mammalian neural stem cells and neurogenesis: five decades later. *Cell Stem Cell.* 2015;17(4):385-395.

27. Kazanis I. The subependymal zone neurogenic niche: a beating heart in the centre of the brain: How plastic is adult neurogenesis? Opportunities for therapy and questions to be addressed. *Brain*, 2009; 132(11):2909-21.

28. Takahashi K, Yamanaka S. Induction of pluripotent stem cells from mouse embryonic and adult fibroblast cultures by defined factors. *Cell.* 2006; 126(4):663-676.

29. Yamanaka S. Strategies and new developments in the generation of patient-specific pluripotent stem cells. *Cell Stem Cell.* 2007; 1(1):39-49.

30. Takahashi K, Tanabe K, Ohnuki M, Narita M, Ichisaka T, Tomoda K, Yamanaka S. Induction of pluripotent stem cells from fibroblast cultures. *Nat Protocols.* 2007a; 2, pp. 663-676.

31. Takahashi K, Tanabe K, Ohnuki M, Narita M, Ichisaka T, Tomoda K, Yamanaka S. Induction of pluripotent stem cells from adult human fibroblasts by defined factors. *Cell.* 2007b; 131(5):861-75.

32. Yu J, Vodyanik MA, Smuga-Otto K, Antosiewicz-Bourget J, Frane JL, Tian S, Nie J, Jonsdottir GA, Ruotti V, Stewart R, Slukvin II, Thomson JA. Induced pluripotent stem cell lines derived from human somatic cells. *Science.* 2007; 318(5858):1917-1920.

33. Karagiannis P, Takahashi K, Saito M, Yoshida Y, Okita K, Watanabe A, Inoue H, Yamashita JK, Todani M, Nakagawa M, Osawa M, Yashiro Y, Yamanaka S, Osafune K. Induced pluripotent stem cells and their use in human models of disease and development. *Physio Rev.* 2019; 99(1):79-114.

34. Robinton DA, Daley GQ. The promise of induced pluripotent stem cells in research and therapy. *Nature*. 2012; 481:295-305.

35. Solder F, Hockemeyer D, Beard C, Gao Q, Bell GW, Cook EG, Hargus G, Blak A, Cooper O, Mitalipova M, Isacson O, Jaenisch R. Parkinson's disease patient-derived induced pluripotent stem cells free of viral reprogramming factors. *Cell.* 2009; 136(5):964-77.

36. Karumbayaram S, Novitch B, Patterson M, Umbach J, Richter L, Lindgren A, Conway A, Clark A, Goldman S, Plath K, Wiedau-Pazos M, Kornblum H, Lowry W. Direct differentiation of human induced pluripotent stem cells generates active motor neurons. *Stem Cells.* 2009; 27(4):806-11.

37. Okada Y, Matsumoto A, Shimazaki T, Enoki R, Koizumi A, Ishii S, Itoyama Y, Sobue G, Okano H. Spatiotemporal recapitulation of central nervous system development by murine embryonic stem cell-derived neural stem/progenitor cells. *Stem Cells.* 2008;26(12):3086-98.

38. Takayama Y, Kida YS. In vitro reconstruction of neural networks derived from human iPS cells using microfabricated devices. *PLoS One.* 2016; 11(2)e0148559.

39. Vierbuchen T, Ostermeier A, Pang ZP, Kokubu Y, Südhof TC, Wernig M. Direct conversion of fibroblasts to functional neurons by defined factors. *Nature*. 2010; 463: 1035-1041.

40. Han DW, Tapia N, Hermann A, Hemmer K, Höing S, Araúzo-Bravo J, Zaehres H, Wu G, Frank F, Moritz S, Greber B, Yang JH, TaekLee H, Schwamborn JC, Storch A, Schöler HR. Direct reprogramming of fibroblasts into neural stem cells by defined factors. *Cell Stem Cell*. 2012; 10(4):465-472.

41. Jones Il, Livi P, Lewandowska MK, Fiscella M, Roscic B, Hierlemann A. The potential of microelectrode arrays and microelectronics for biomedical research and diagnostics. *Anal Bioanal Chem.* 2011; 399(7):2313-29.

42. Malerba M, Amin H, Angotzi GN, Maccione A, Berdondini L. Fabrication of multielectrode arrays for neurobiology applications. *Methods Mol Biol.* 2018; 1771:147-157.

43. Johnston AF, Gross GW, Weiss DG, Schroeder OH, Gramowski A, Shafer TJ. Microelectrode arrays: a physiologically based neurotoxicity testing platform for the 21st century. *Neurotoxicology.* 2010;31(4):331-50.

44. Simão D, Silva MM, Terrasso AP, Arez F, Sousa MF, Mehrjardi NZ, Šarić T, Gomes-Alves P, Raimundo N, Alves PM, Brito C. Recapitulation of human neural microenvironment signatures in iPSC-derived NPC 3D differentiation. *Stem Cell Reports.* 2018; 11(2):552-64.

45. Wang XF, Cynader MS. Effects of astrocytes on neuronal attachment and survival shown in a serum-free-co-culture system. *Brain Res Brain Res Protoc.* 1999; 4(2):209-16.

46. Aebersold MJ, Thompson-Steckel G, Joutang A, Schneider M, Burchert C, Forró C, Weydert S, Han H, Vörös J. Simple and inexpensive paper-based astrocyte co-culture to improve survival of low-density neuronal networks. *Front Neurosci.* 2018; 12.

47. Ricci G, Volpi L, Pasquali L, Petrozzi L, Siciliano G. Astrocyte neuron interactions in neurological disorders. *J Bio Phys.* 2009;35(4):317-336.

48. Kettenmann H, Verkhratsky A. Neuroglia: the 150 years after. *Trends Neurosci.* 2008;31(12):653-9.

49. Barker AJ, Ullian EM. New roles for astrocytes in developing synaptic circuits. *Commun Integr Biol.* 2008;1(2): 207-11.

50. Chung WS, Allen NJ, Eroglu C. Astrocytes control synapse formation, function and elimination. *Cold Spring Harb Perspect Biol.* 2015;7(9).

51. Ullian EM, Sapperstein SK, Christopherson KS, Barres BA. Control of synapse number by glia. *Science.* 2001; 291(5504):657-61.

52. Katz LC, Shatz CJ. Synaptic activity and the construction of cortical circuits. *Science.* 1996; 274(5290):1133-1138.

53. Ben-Ari Y. Developing networks play a similar melody. *Trends Neurosci.* 2001; 24(6):353-60.

54. Kirwan P, Turner-Bridger B, Peter M, Momoh A, Arambepola D, Robinson HP, Livesey FJ. Development and function of human cerebral cortex neural networks from pluripotent stem cells in vitro. *Development.* 2015; 142(18):3178-87.

55. Triplett MA, Avitan L, Goodhill GJ. Emergence of spontaneous assembly activity in developing neural networks without afferent input. *PLoS Comput Biol.* 2018; 14(9): e1006421.

56. Chiappalone M, Vato A. Network dynamics and synchronous activity in cultured cortical neurons. *Int J Neural Syst.* 2007; 17(2):87-103.

57. Salinas E, Sejnowski TJ. Correlated neuronal activity and the flow of neural information. *Nat Rev Neurosci.* 2001; 2 (8):539-50.

58. Odawara A, Saitoh Y, Alhebshi AH, Gotoh M, Suzuki I. Long-term electrophysiological activity and pharmacological response of a human induced pluripotent stem cell-derived neurons and astrocyte co-culture. *Biochem Biophys Res Commun.* 2016; 443(4):1176-81.

59. Amin H, Maccione A, Marinaro F, Zordan S, Nieus T, Berdondini L. Electrical responses and spontaneous activity of human iPSC-derived neuronal networks characterized for 3-month culture with 4096- electrode arrays. *Front Neurosci.* 2016; 10: 121. doi: 10.3389/fnins.2016.00121.

60. Khazipov R, Sirota A, Leinenkugel X, Holmes GL, Ben-Ari Y, Buzáki G. Early motor activity drives spindle bursts in the developing somatosensory cortex. *Nature.* 2004; 432:758-761.

61. Kilb W, Kirischuk S, Luhmann HJ. Electrical activity patterns and the functional maturation of the neocortex. *Eur J Neurosci.* 2011;34(10):1677-86.

62. Leinenkugel X, Khazipov R, Cannon R, Hirase H, Ben-Ari Y, Buzáki G. Correlated bursts of activity in the neonatal hippocampus *in vivo. Science.* 2002; 296(5575):2049-2052.

63. Khazipov R, Luhmann HJ. Early patterns of electrical activity in the developing cerebral cortex of humans and rodents. *Trends Neurosci.* 2006; 29(7):414-418.

64. Moore AR, Zhou WL, Jakovcevski I, Zecevic N, Antic SD. Spontaneous electrical activity in the human fetal cortex *in vitro. J Neurosci.* 2011; 31(7):2391-2398.

65. Tolonen M, Palva JM, Andersson S, Vanhatalo S. Development of the spontaneous activity transients and ongoing cortical activity in human preterm babies. *Neuroscience.* 2006; 145(3):997-1006.

66. Corlew R, Bosma MM, Moody WJ. Spontaneous, synchronous electrical activity in neonatal mouse cortical neurones. *J Physiol*. 2004; 15; 560(Pt 2): 377-390.

67. Kapucu FE, Tanskanen JM, Mikkonen JE, Ylä-Outinen L, Narkilahti S, Hyttinen JA. Burst analysis tool for developing neuronal networks exhibiting highly varying action potential dynamics. *Front Comput Neurosci*. 2012; 6:38. doi: 10.3389/fncom.2012.00038

68. Lisman JE. Bursts as a unit of neural information: making unreliable synapses reliable. *Trends Neurosci.* 1997; 20(1):38-43

69. Maeda E, Kuroda Y, Robinson HP, Kawana A. Modification of parallel activity elicited by propagating bursts in developing networks of rat cortical neurones. *Eur J Neurosci.* 1998;10(2):488-96.

70. Jimbo Y, Tateno T, Robinson HP. Simultaneous induction of pathway-specific potentiation and depression in networks of cortical neurons. *Biophys J.* 1999;76(2):670-8.

71. Shahaf G, Marom S. Learning in networks of cortical neurons. *J Neurosci.* 2001;21(22):8782-8.

72. Le Feber J, Stegenga J, Rutten WL. The effect of slow electrical stimuli to achieve learning in cultured networks of rat cortical neurons. *PLoS One.* 2010;5(1): e8871.

73. Lee HK, Kameyama K, Huganir RL, Bear MF. NMDA induces long-term synaptic depression and dephosphorylation of the GluR1 subunit of AMPA receptors in hippocampus. *Neuron.* 1998; 21(5):1151-62.

74. Lee HK, Barbarosie M, Kameyama K, Bear MK, Huganir RL. Regulation of distinct AMPA receptor phosphorylation sites during bidirectional synaptic plasticity. *Nature.* 2000; 405(6789):955-959.

75. Bi GQ, Poo MM. Synaptic modifications in cultured hippocampal neurons: dependence on spike timing, synaptic strength, and postsynaptic cell type. *J Neurosci.* 18(24):10464-72.

76. Nelson SB, Turrigiano GG. Strength through diversity. *Neuron.* 2008; 60(3):477-82.

77. Roberson ED, English JD, Sweatt JD. A biochemist's view of long-term potentiation. *Learn Mem.* 1996; 3(1):1-24.

78. Villers A, Godaux R, Ris L. Long-lasting LTP requires neither repeated trains for its induction nor protein synthesis for its development. *PLoS ONE.* 2012; 7(7): e40823.

79. Sweatt JD. Neural plasticity and behaviour- sixty years of conceptual advances. *J Neurochem.* 2016; 139 Suppl 2: 179-199.

80. Nicoll RA, Malenka RC. Expression mechanisms underlying NMDA receptor-dependent long-term potentiation. *Ann N Y Acad Sci.* 1999; 868:515-25.

81. Malinow R, Madison DV, Tsien RW. Persistent protein kinase activity underlying long-term potentiation. *Nature.* 1988; 335(6193):820-4.

82. Chater TE, Goda Y. The role of AMPA receptors in postsynaptic mechanisms of synaptic plasticity. *Front Cell Neurosci.* 2014; 8:401. doi: 10.3389/fncel.2014.00401

83. Keck T, Toyoizumi T, Chen L, Doiron B, Feldman DE, Fox K, Gerstner W, Haydon PG, Hubener M, Lee HK, Lisman JE, Rose T, Sengpiel F, Stellwagen D, Stryker MP, Turrigiano GG, van Rossum MC. Integrating Hebbian and homeostatic plasticity: the current state of the field and future research directions. *Philos Trans R Soc Lond B Biol Sci.* 2017; 372(1715).

84. Fernandes D, Carvalho AL. Mechanisms of homeostatic plasticity in the excitatory synapse. *J Neurochem.* 2016;139(6):973-996.

85. Hobbiss AF, Ramiro-Cortes Y, Israely I. Homeostatic plasticity scales dendritic spine volumes and changes the threshold and specificity of Hebbian plasticity. *iScience.* 2018; 8:161-74.

86. Zenke F, Gerstner W. Hebbian plasticity requires compensatory processes on multiple timescales. *Philos Trans R Soc Lond B Biol Sci.* 2017; 372(1715).

87. Zenke F, Gerstner W, Ganguli S. The temporal paradox of Hebbian learning and homeostatic plasticity. *Curr Opin Neurobiol.* 2017; 43:166-176.

88. Bastrikova N, Gardner GA, Reece JM, Jeromin A, Dudek SM. Synapse elimination accompanies functional plasticity in hippocampal neurons. *Proc Natl Acad Sci. USA.* 2008: 3123-3127.

89. Pozo K, Goda Y. Unraveling mechanisms of homeostatic synaptic plasticity. *Neuron*. 2010;66(3):337-351.

90. Chowdhury D, Hell JW. Homeostatic synaptic scaling: molecular regulators of synaptic AMPA-type glutamate receptors. *F1000Res*. 2018; 7:234. doi:10.12688/f1000research.13561.1

91. Yee AX, Hsu YT, Chen L. A metaplasticity view of the interaction between homeostatic and Hebbian plasticity. *Phil. Trans. R. Soc. Bio Sci.* 2017; 372(1715): 20160155.

92. Bienenstock EL, Cooper LN, Munro PW. Theory for the development of neuron selectivity, orientation specificity and binocular interaction in visual cortex. *J. Neurosci.* 1982; (1):32-48.

93. Turrigiano GG, Nelson SB. Hebb and homeostasis in neuronal plasticity. *Curr Opin Neurobiol.* 2000; 10(3):358-64.

94. Turrigiano GG. The dialect of Hebb and homeostasis. *Philos Trans R Soc Lond B Bio Sci.* 2017; 372(1715).

95. Lewitus GM, Konefal SC, Greenhalgh AD, Pribiag H, Augereau K, Stellwagen D. Microglial TNF-α suppresses cocaine-induced plasticity and behavioral sensitization. *Neuron* 2016; 90*,* 483–491*.*

96. Lewitus GM, Pribiag H, Duseja R, St-Hilaire M, Stellwagen D. An adaptive role of TNFα in the regulation of striatal synapses. *J. Neurosci*. 2014; (34):6146–6155.

97. Stellwagen D, Malenka RC. Synaptic scaling mediated by glial TNF-alpha. *Nature.* 2006; 440:1054–1059.

98. Bridi MCD, de Pasquale R, Lantz CL, Gu Y, Borrell A, Choi SY, He K, Tran T, Hong SZ, Dykman A, Lee HK, Quinlan EM, Kirkwood A. Two distinct mechanisms for experience-dependence homeostasis. *Nat Neurosci.* 2018;21(6):843-850.

99. Henderson JA, Gong P. Functional mechanisms underlie the emergence of a diverse range of plasticity phenomena. *PLoS Comput Biol.* 2018;14(11). Wierenga CJ, Ibata K, Turrigiano GG. Postsynaptic expression of homeostatic plasticity at neocortical synapses. J Neurosci. 2005; 25(11):2895-905.

100. Wierenga CJ, Ibata K, Turrigiano GG. Postsynaptic expression of homeostatic plasticity at neocortical synapses. *J Neurosci.* 2005; 25(11):2895-905.

101. Ibata K, Sun Q, Turrigiano GG. Rapid synaptic scaling induced by changes in postsynaptic firing. *Neuron.* 2008; 57(6):819-26.

102. Vitureira N, Goda Y. Cell biology in neuroscience: the interplay between Hebbian and homeostatic plasticity. *J Cell Biol.* 2013: 203(2):175-86.

103. Henning MH. Theoretical models of synaptic short term plasticity. *Front. Comput. Neurosci.* 2013; 7(45)

104. Kettenmann H, Verkhratsky A. Neuroglia-living nerve glue. *Fortschr Neurol Psychiatr.* 2011; 79(10):588-97.

105. Minoura I. Towards an understanding of the isotype-specific functions of tubulin in neurons: technical advances in tubulin expression and purification. *Neurosci Res.* 2017; 1-8. Doi: 10.1016/j.neures.2017.04.002.

106. Harris KP, Littleton JT. Transmission, development and plasticity of synapses. *Genetics.* 2015;201(20:345-375.

107. Mauch DH, Nagler K, Scumacher S, Goritz C, Muller EC, Otto A, Pfrieger FW. CNS synaptogenesis promoted by glia-derived cholesterol. *Science.* 2001;294(5545):1354-1357.

108. Abney ER, Bartlett PP, Raff MC. Astrocytes, ependymal cells, and oligodengrocytes develop on schedule in cell sultures of embryonic rat brain. *Dev. Biol.* 1981;83: 301-310.

109. Qian X, Shen Q, Goderie SK, He W, Capela A, Davis AA, Temple S. Timing of CNS cell generation: a programmed sequence of neuron and glial cell production from isolated murine cortical stem cells. *Neuron.* 2000;28(1):69-80.

110. Pfrieger FW, Barres BA. Synaptic efficacy enhanced by glial cells in vitro. *Science.* 1997; 277 (5332): 1684-1687

111. Zhan X, Lai PY, Chan CK. Effects of glial release and somatic receptors on bursting in synchronized neuronal networks. *Phys Rev.* 2011; 84(1): 011907.

112. Halassa MM, Haydon PG. Integrated brain circuits: astrocytic networks modulate neuronal activity and behavior. *Annu Rev Physiol*. 2012; 72:335-55.

113. Bradford AB, McNutt PM. Importance of being Nerst: synaptic activity and functional relevance in stem cell-derived neurons. *World J Stem Cells.* 2015; 7(6): 899-921.

114. Latham PE, Richmond BJ, Nelson PG, Nirenberg S. Intrinsic dynamics in neuronal networks. I. Theory. *Neurophysiol.* 2000;83(2):808-27.

115. Krahe R, Gabbiani F. Burst firing in sensory systems. *Nat Rev Neurosci.* 2004; 5:13-23.

116. Masquelier T, Deco G. Network bursting dynamics in excitatory cortical neuron cultures results from the combination of different adaptive mechanisms. *PLoS One.* 2013; 8(10): e75824.

117. Eytan D, Marom S. Dynamics and effective topology underling synchronization in networks of cortical neurons. *J Neurosci*. 2006; 26(33): 8465-8476.

118. Stephens CL, Toda H, Palmer TD, DeMarse TB, Ormerod BK. Adult neural progenitor cells reactivate superbursting in mature neural networks. *Experi Neuro.* 2012; 234(1):20-30.

119. Izhikevich EM, Desai NS, Walcott EC, Hoppensteadt FC. Bursts as a unit of neural information: selective communication via resonance. *Trends Neurosci.* 2003; 26(3):161-7.

120. Huang YT, Chang YL, Chen CC, Lai PY, Chan CK. Positive feedback and synchronized bursts in neuronal cultures. *PLoS ONE.* 2017; 12(11): e0187276.

121. Fetz EE. Temporal coding in neural populations? *Science.* 1997; 279(5345): 1901-1902.

122. Abraham WC. How long will long term potentiation last? *Philos Trans R Soc Lond B Biol Sci.* 2003; 358(1432):735-744.

123. Aertsen A, Diesmann M, Gewaltig MO. Propagation of synchronous activity in feedforward neural networks. *J Physiol Paris.* 1996; 90(3-4): 243-7.

124. Yee AX, Hsu YT, Chen L. A meteplasticity view of the interaction between homeostatic and Hebbian plasticity. *Phil. Trans. R. Soc. B.* 2017; 372:20160155.

125. Hennig MH. Theoretical models of synaptic short-term plasticity. *Front Comput Neurosci.* 2013: 7(45).

126. Pozo, K, & Goda, Y. Unraveling mechanisms of homeostatic synaptic plasticity. *Neuron*. *2010; 66*(3), 337–351.

127. Kitano H. Biological robustness. *Nat Rev Genet.* 2004; 5(11):826-37.

128. Roth BL. DREADDs for neuroscientists. *Neuron.* 89(4):683-694.

129. Smith KS, Bucci DJ, Luikart BW, Mahler SV. DREADDS: use and application in behavioral neuroscience. *Behav Neurosci.* 2016; 130(2):137-55.

130. Van Huizen F, Romijin HJ, Habets AM. Synaptogenesis in rat cerebral cortex cultures is affected during chronic blockade of spontaneous bioelectric activity by tetrodotoxin. *Brain Res.* 1985; 351(1):67-80.

131. Van Huizen F, Romijin HJ, Habets AM, van den Hooff P. Accelerated neural network formation in rat cerebral cortex cultures chronically disinhibited with picrotoxin. *Exp Neurol.* 1987; 97(2):280-8.

132. Stett A, Egert U, Guenther E, Hofmann F, Meyer T, Nisch W, Haemmerie H. Biological application of microelectrode arrays in drug discovery and basic research. *Anal Bioanal.* 2003;377(3):486-95.

11. APPENDIX

11.1 A pilot design for chemogenetic modulation of *in vitro* neural networks

11.1.1 The 60 electrode-6 well MEA platform

The 60 electrode-6well (60-6well) MEAs (*Multi-Channel System MCS GmbH*) has a macrolon ring with 6 separate triangular chambers that allows for recording/stimulation of six separate networks simultaneously. Inside each chamber is a field of 9 electrodes with an internal reference electrode. The electrodes and contact pads are made of titanium nitride (TiN), the isolation is made up of Silicon nitride (SiN), while the tracks are from titanium (Ti). As with the standard MEA, the diameter of the electrodes is 30 µm and the distance from center to center is 200 µm.

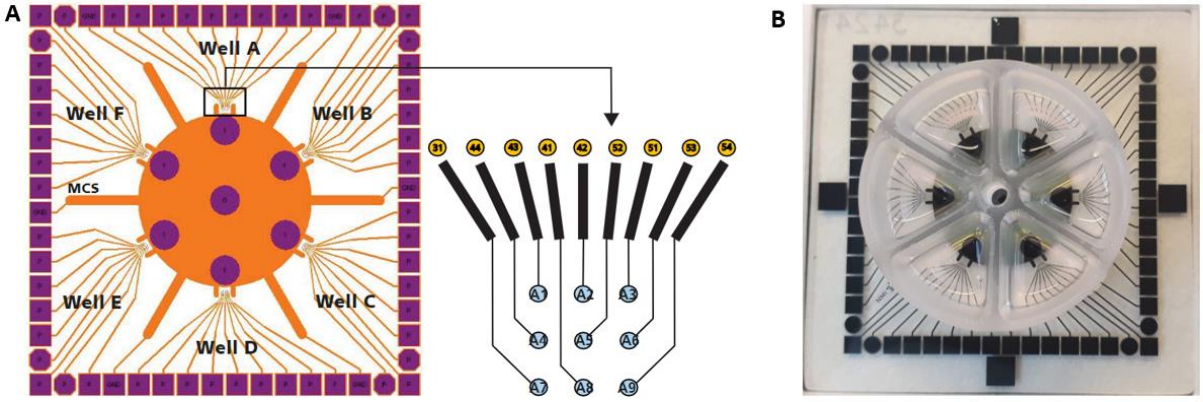

Appendix Fig 1. *A) Each well is identified by a letter and each electrode in each well is numbered with the letter identifier. The letter-digit code identifies the electrode and refers to the position in the well. B) 60-6well MEA 200/30 iR Ti MEA. Each ring chamber has a volumetric capacity of 700µl.*

11.1.2 Example set up for neuronal populations transfected with DREADDs on MEAs (n=2)

hiPSC-derived neurons can be transfected with DREADDs proteins (pAAV-CaMKIIa -*Gq* hM3D and pAAV-CaMKIIa-*Gi* hM4D). Each compartment on the MEA will have a different population of transfected cells, as well as non-transfected cells (normal). This may lead to interesting comparability among populations. Since the wells are completely separated from each other, the hypothesis is that the neurons in each well should produce a distinctly different pattern of electrophysiological activity.

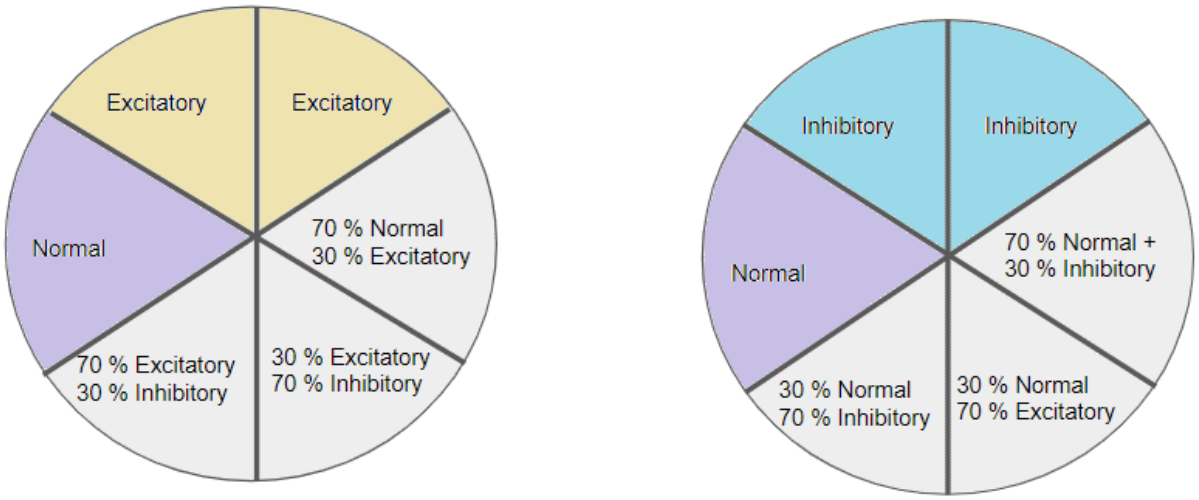

Appendix Fig 2. Preliminary schematic of the seeding organization of hiPSC-derived neurons transfected with DREADDs on two 60-6well MEAs. *For each MEA, three wells will contain single population of cells, either non-transfected cells (normal) or cells transfected with the inhibitory plasmid or excitatory plasmid. The remaining wells will have mixed population of cells at different seeding densities.*

12. SUPPLEMENTARY

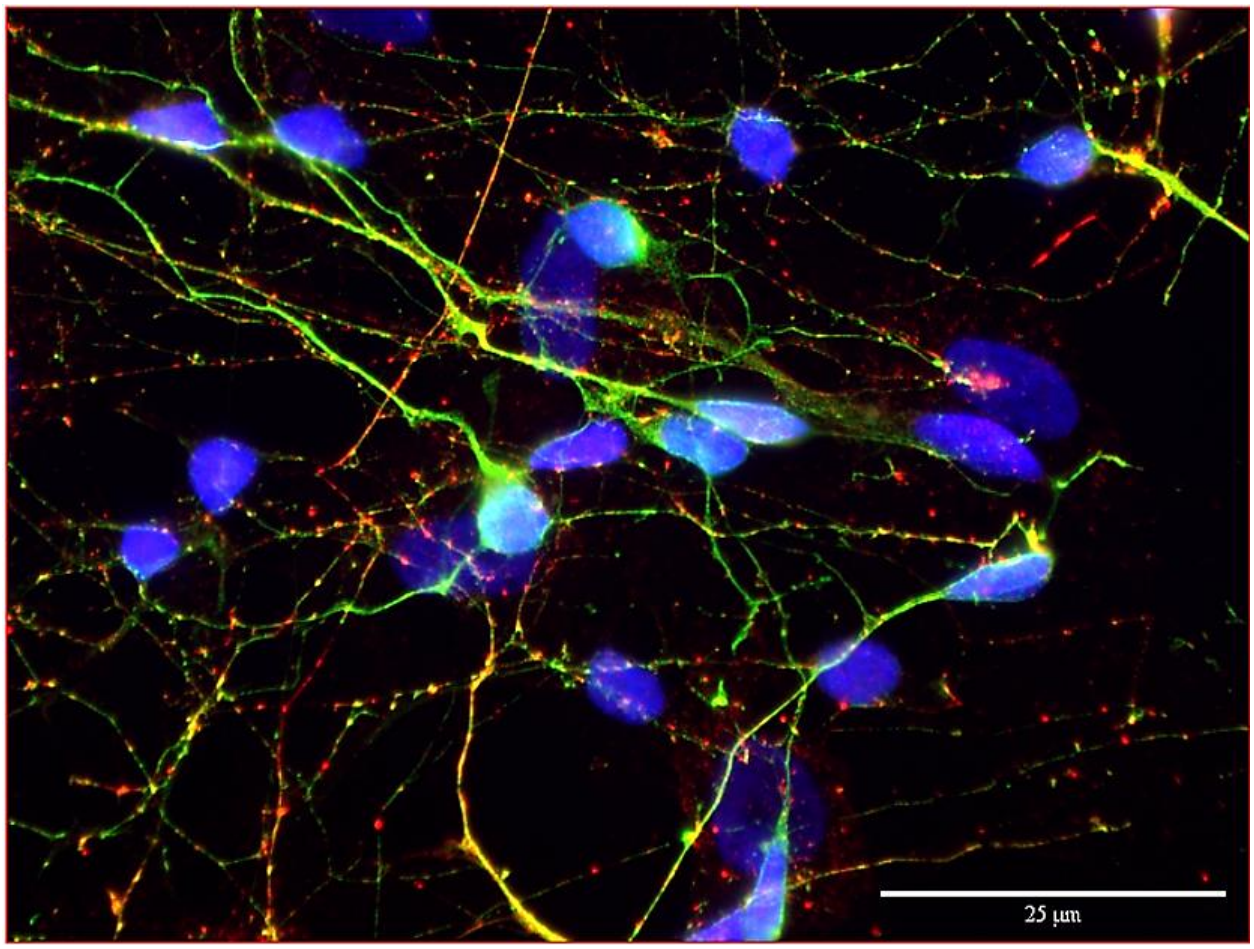

Supplementary Fig 1. Immunocytochemistry against neuron specific markers at 14 DIV. *The cell bodies are stained with DAPI (blue). Extensive process arborization can be visualized here with TUJ (green) and pre-synaptic areas are visualized with synaptophysin (red). Magnification 100X. Scale bar 25µm.*

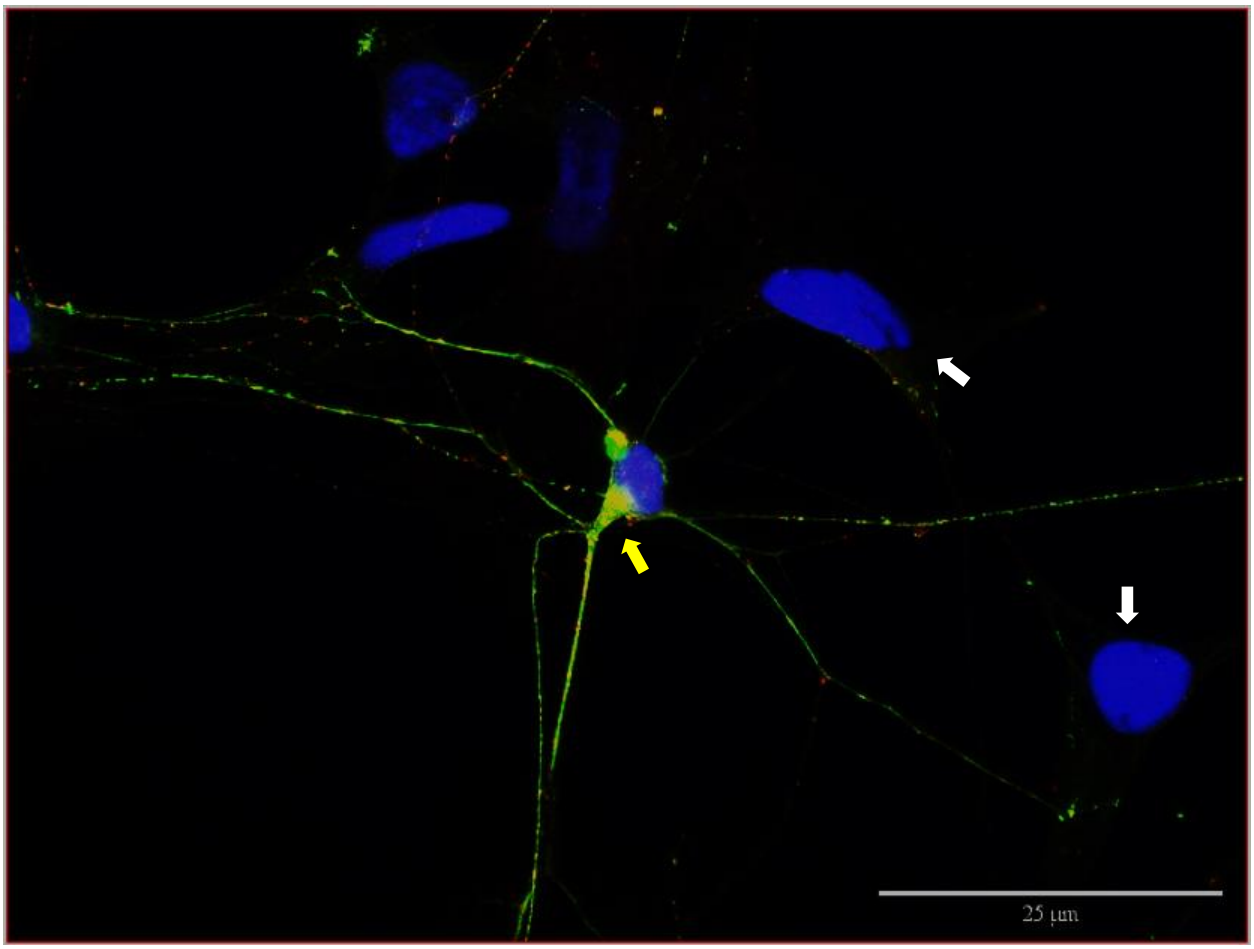

Supplementary Fig 2. Immunocytochemistry against neuron specific markers at 14 DIV. *The areas highlighted by the white arrows appear to be the somata of astrocytes. The yellow arrow highlights what appears to be the axon hillock of the neuron. DAPI (blue), TUJ (green), Synaptophysin (Red). Magnification 100X. Scale bar 25µm.*

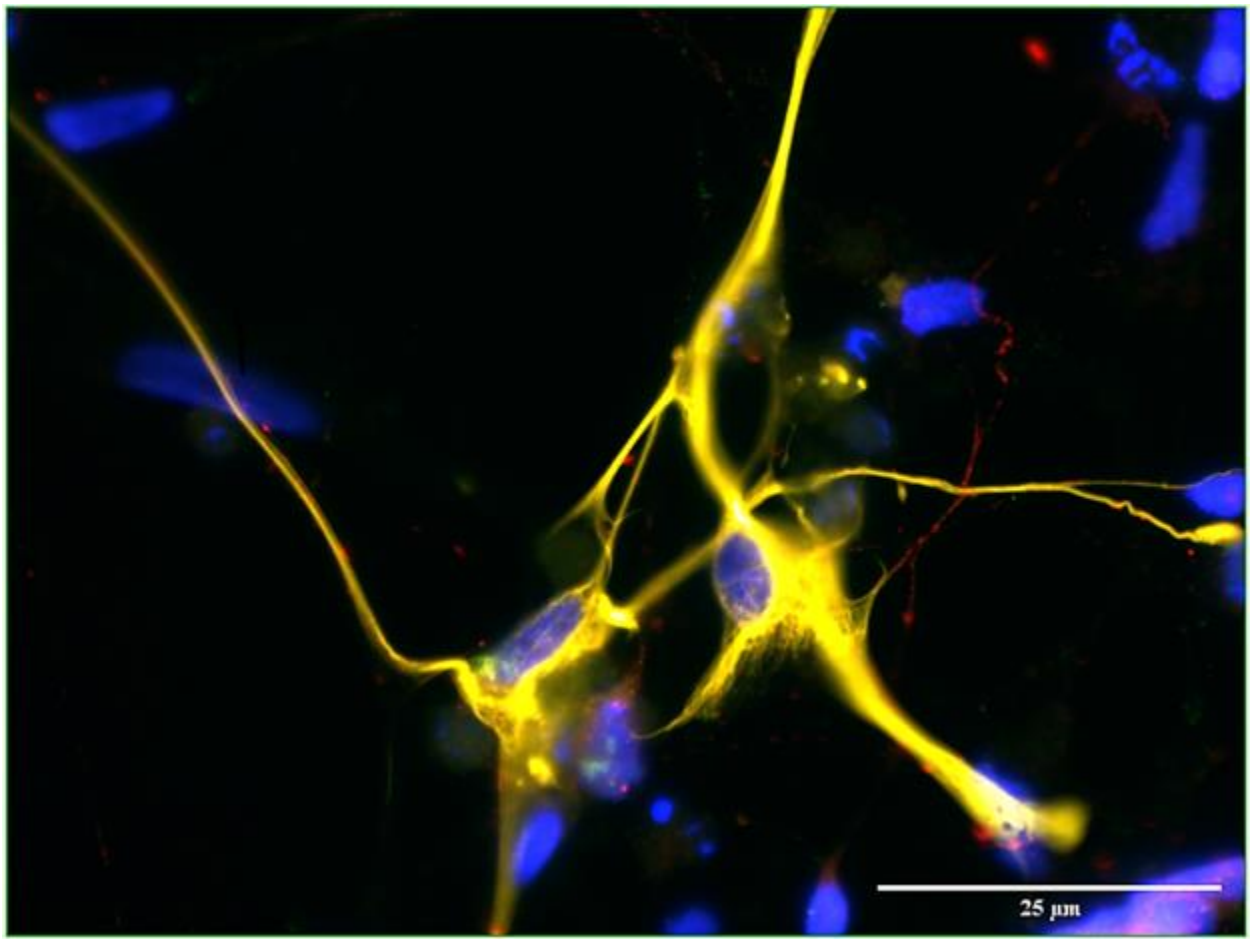

Supplementary Fig 3. Immunocytochemistry depicting astrocytes. *DAPI (blue), GFAP (yellow), Synaptophysin (red), PSD-95 (green). Magnification 100X. Scale bar 25µm.*

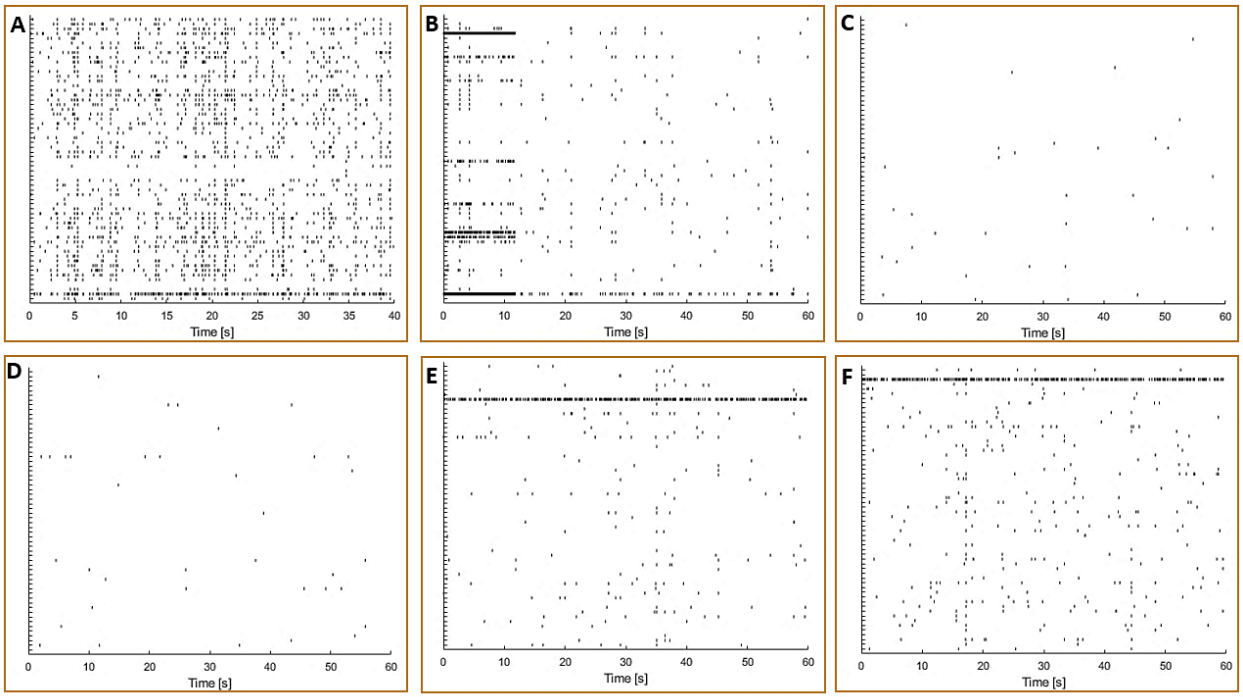

Supplementary Fig 4. Spontaneous electrical activity for (in vitro neural) Network 1. *Recorded LFP (spike) is depicted as a single vertical line. The horizontal ticks on the y-axis are the recording channels and each represent the spike train recording for one electrode. The darker areas where the spikes occurred together may be considered bursts. The x-axis is the time in seconds for the duration of the recording period (60 seconds of the total 3 minutes recording). (A) 09 DIV; (B) 15 DIV; (C) 28 DIV; (D) 40 DIV (E) 44 DIV; (F) 50 DIV*

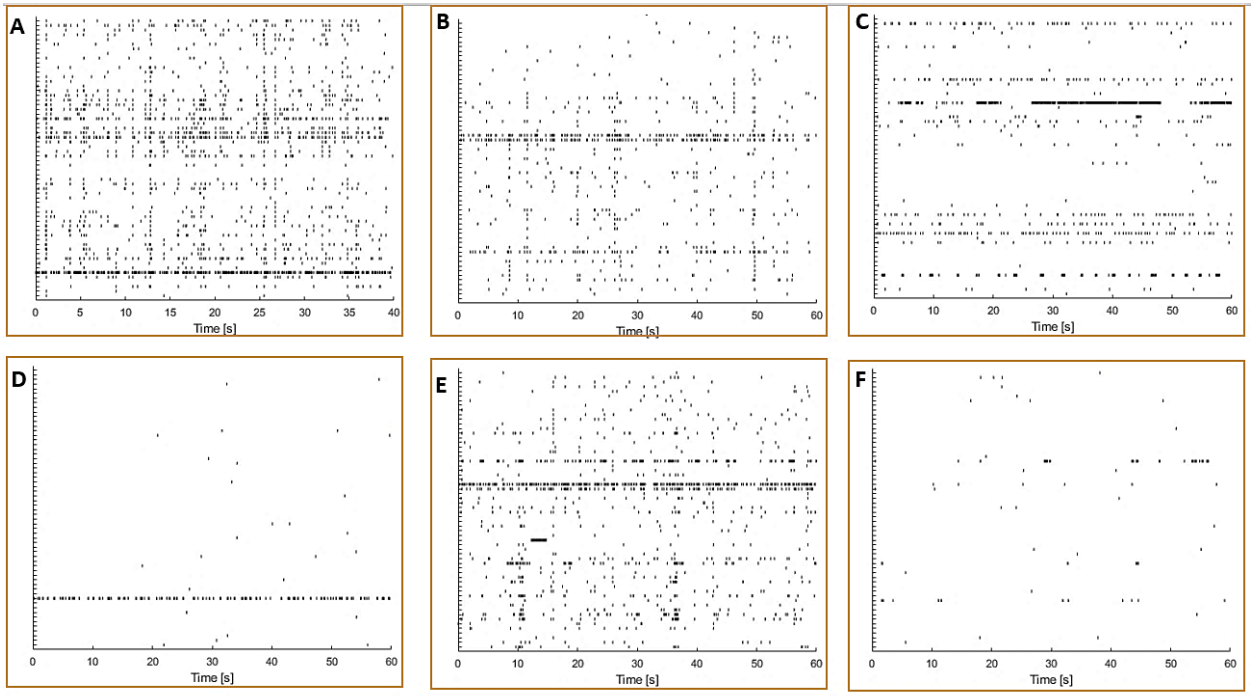

Supplementary Fig 5. Spontaneous electrical activity for (in vitro neural) Network 2. *Recorded LFP (spike) is depicted as a single vertical line. The horizontal ticks on the y-axis are the recording channels and each represent the spike train recording for one electrode. The darker areas where the spikes occurred together may be considered bursts. The x-axis is the time in seconds for the duration of the recording period (60 seconds of the total 3 minutes recording). (A) 09 DIV; (B) 15 DIV; (C) 28 DIV; (D) 40 DIV (E) 44 DIV; (F) 50 DIV*

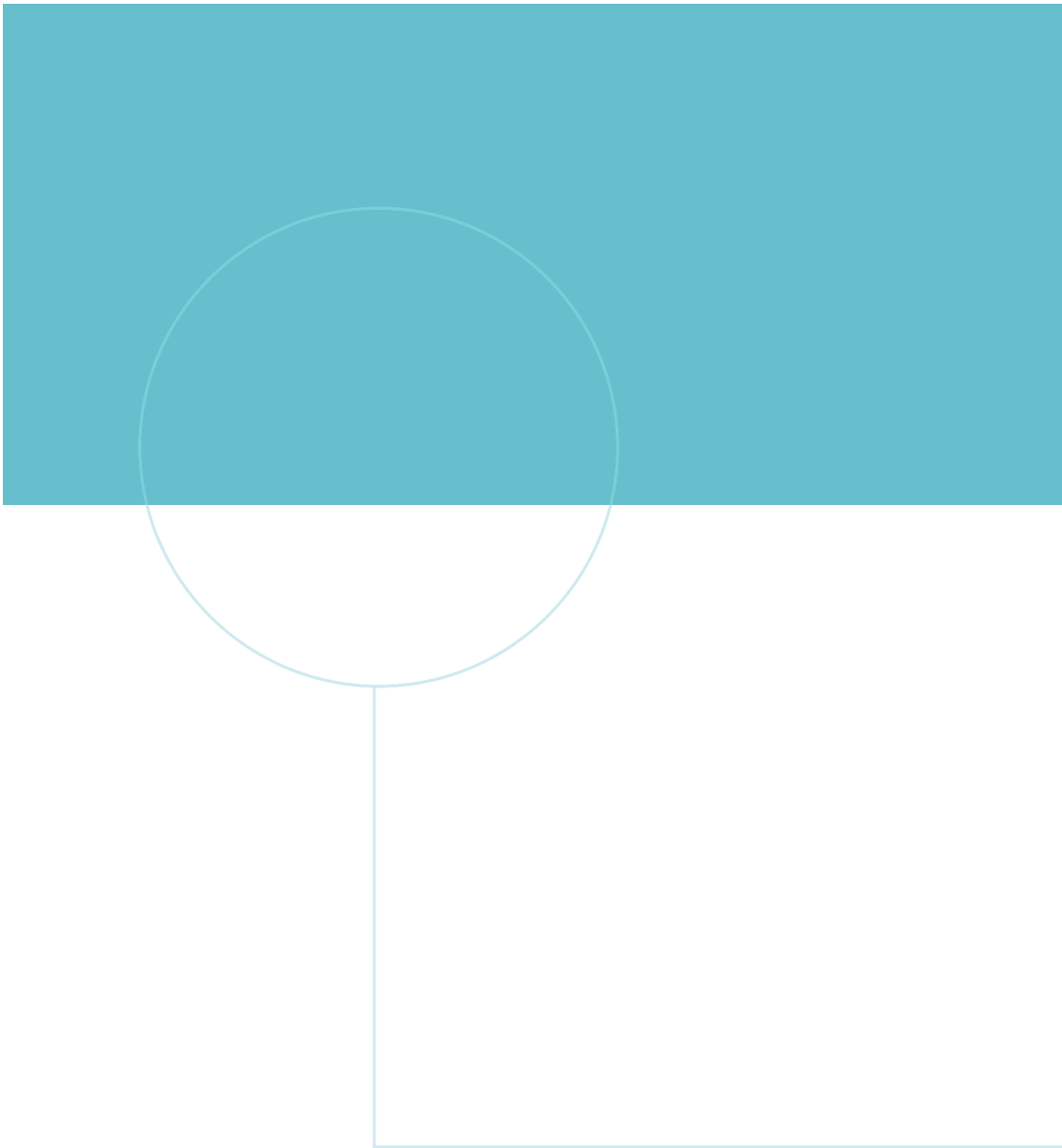

NTNU

Kunnskap for en bedre verden